



FAMU-FSU  
Engineering

# **Performance Testing of GRS Test Piers Constructed with Florida Aggregates - Axial Load Deformation Relationships (BED30 977-11)**

Principal Investigator: Scott Wasman, Ph.D.

Project Managers: Larry Jones, P.E. (Retired)

Rodrigo Herrera, P.E.

Graduate Assistant: Christian Matemu, Ph.D.

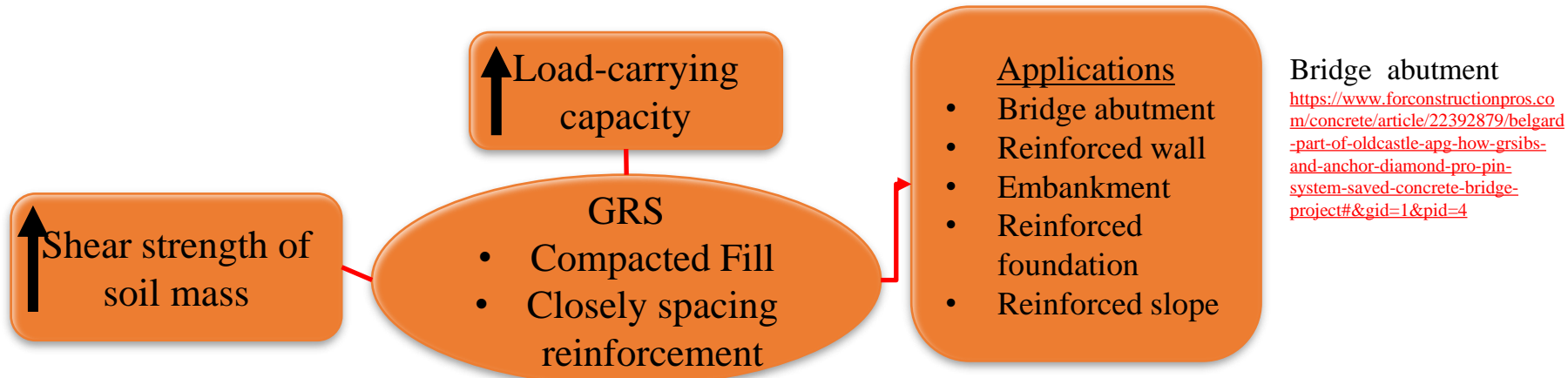
Project Closeout Meeting

August 15<sup>th</sup>, 2024

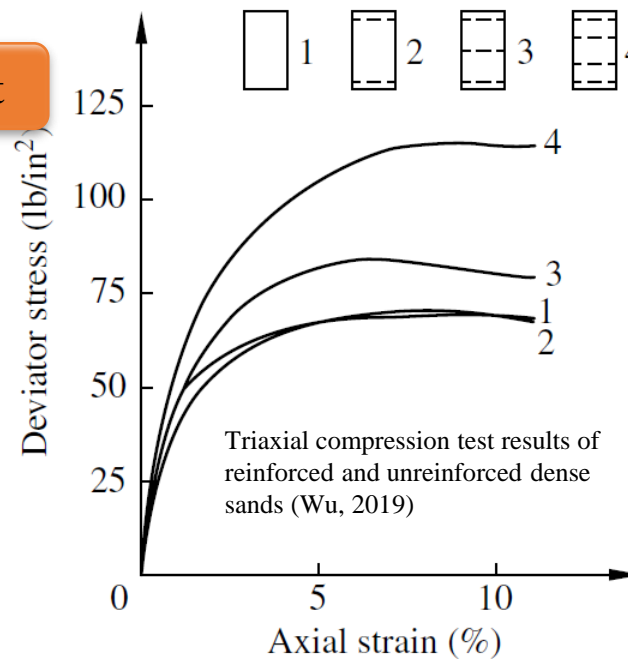
## Presentation Outline

- Background and Motivation
- Project Objectives and Tasks
- Research Findings
- Research Conclusions
- Recommendations

# Background: Geosynthetic Reinforced Soil (GRS)



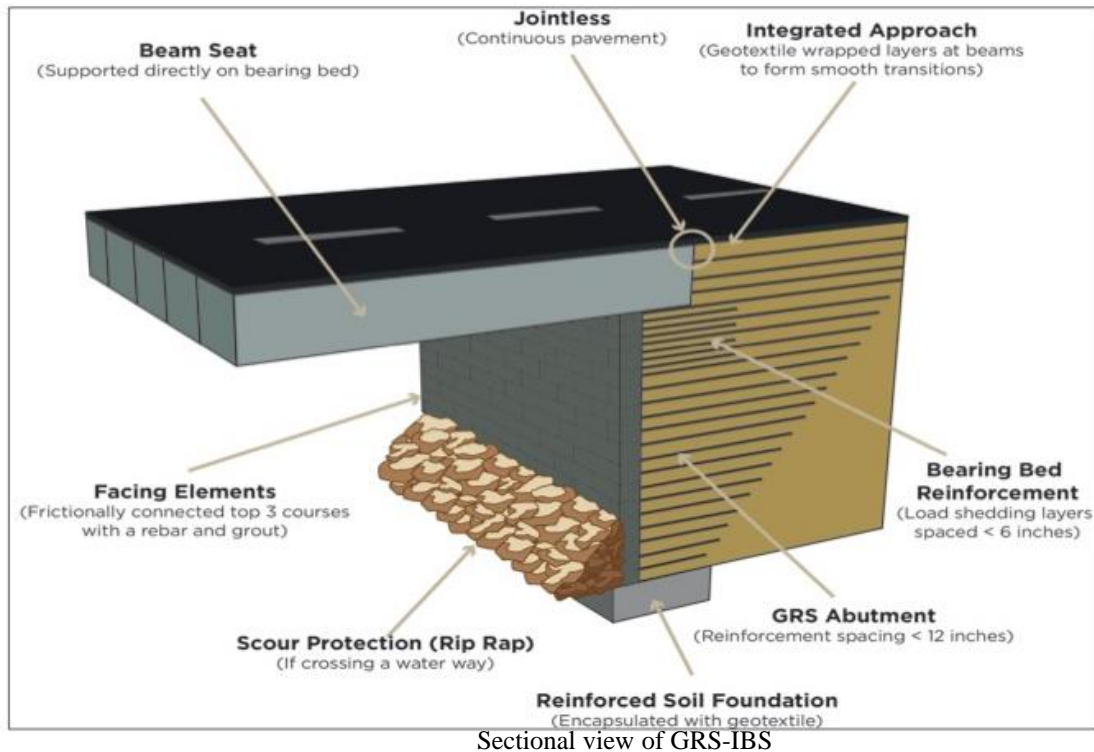
- **Reinforcement**
  - Provides tensile strength
- **Behavior**
  - Backfill properties
  - Reinforcement properties
  - Vertical spacing
  - Facing conditions



Reinforced slope

## Background: What is GRS-IBS?

- FHWA promoted its use to Geosynthetic Reinforced Soil Integrated Bridge system (GRS-IBS):
  - Saving time and cost, eliminates “bump at bridge” problem, flexible design, flexible design



Construction of U.S. 301 Trail Bridge with multi-span GRS-IBS in Zephyrhills, Florida (Danilyarov et al., 2017)



Single span <140 ft  
Abutment height <30 ft  
Service limit pressure 4 ksf

>300 bridges with  
GRS-IBS in USA

Orange Avenue Bridge in Tallahassee, Florida  
<https://ncma.org/updates/projects/florida-manages-orange-avenue-bridge-with-grs-ibs/>

# Research Motivation

## Facing

- FHWA, CMU
- FDOT, SRB ??

## Reinforcement

- FHWA,  $T_f \leq 4,800$  lb/ft
- FDOT  $T_f \geq 4,800$  lb/ft ??

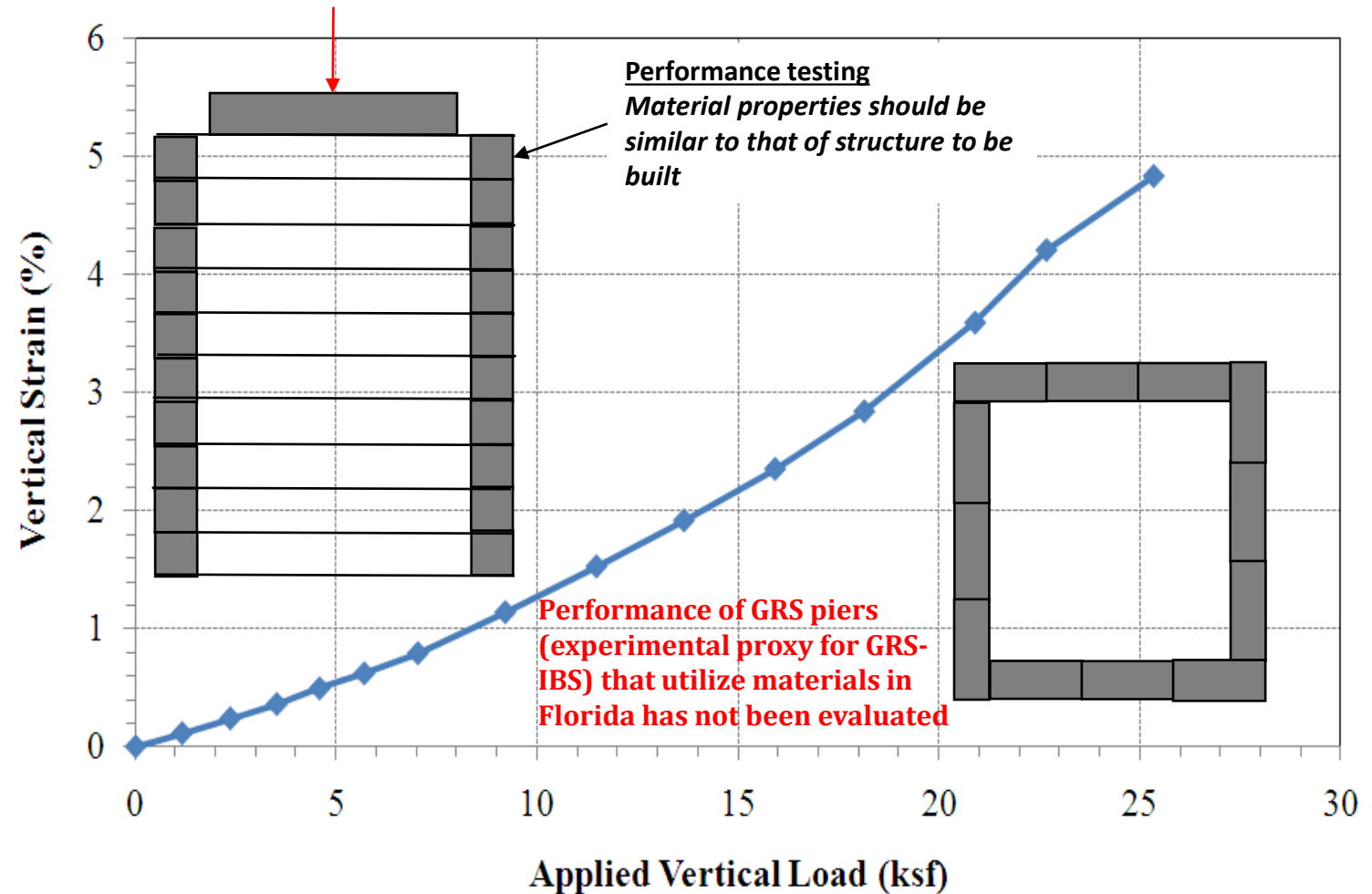
## Performance of GRS

## Backfill

- Florida aggregates ??
- Other Materials i.e. FGA??

Axial load at FHWA Service limits  
 $\epsilon_v = 1\%$  and  
 $\epsilon_H = 2\%$  ??

Property	# 57 Florida	#57 Virginia
	Limestone	Limestone
LA Abrasion Loss (5)	38	23
Friction angle (deg)	44.8 <sup>SDTX</sup>	40.5 <sup>LDTX</sup>
Max Density	96	108.7
Min Density	82	95.4



SDTX based on small diameter (4") triaxial test  
 LDTX based on large diameter (6") triaxial test

Design envelope (Adams et al., 2012)

## Project Objectives and Tasks

- Perform full-scale axial load-deformation tests on 8-GRS piers constructed with FDOT approved aggregates, geosynthetics, and facing blocks.
- Identify service limits ( $\varepsilon_v = 1\%$  and  $\varepsilon_H = 2\%$ ) and vertical bearing capacity.
- Measure aggregate strength properties with large diameter triaxial tests.
- Compare findings to existing test results by FHWA.
- Add to existing FHWA vertical bearing capacity dataset for LRFD.

## Project Tasks

- Task-1: Review previous studies on GRS, design methods, material, and construction practices
- Task-2: Design experimental plan for performance tests
- Task-3: Performance tests – Axial load-deformation tests on GRS piers
- Task-4: Compare performance test results with previous results and predictions and make recommendations for GRS design in Florida
- Task-5: Draft final report and closeout teleconference
- Task 6: Final report

## Task 1: Review previous studies on GRS, design methods, material, and construction practices

- FDOT requires LRFD design of GRS-IBS according to “***Geosynthetic Reinforced Soil Integrated Bridge System Interim Implementation Guide***” FHWA-HRT-11-026, except as otherwise shown in the *FDOT Structures Design Guidelines*.
- Materials
  - Backfill
    - $d_{max} = 2 \text{ inches}$ ,  $\Phi_{min} = 42^\circ$
    - Poorly graded No. 57
    - Well graded GAB
  - Reinforcement
    - Woven polypropylene geotextiles:  $T_{f,min} = 4,800 \text{ lb/ft}$
    - $S_{vmin}$  = lessor of 8 inches or height of facing blocks
  - Facing
    - Segmental retaining blocks (SRB)
- Approximately 20 GRS pier tests performed prior to this project
- A few GRS-IBS built with lightweight foamed glass aggregate (FGA)

# Task 1: Review previous studies on GRS, design methods, material, and construction practices

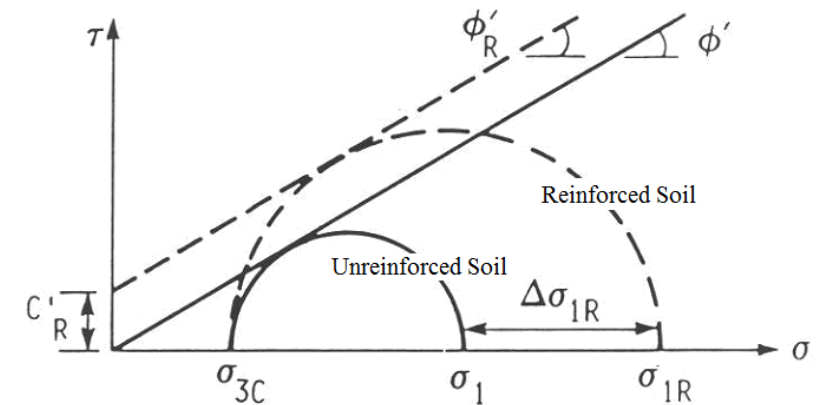
## • A: Bearing Capacity

- Based on Pham (2009) and Wu et al. (2013) work
  - Concept of apparent cohesion
  - Concept of apparent confining pressure
- Doesn't account
  - Presence of bearing bed reinforcement
  - Behavior at the soil and geosynthetic interface
  - Particle size applicability??

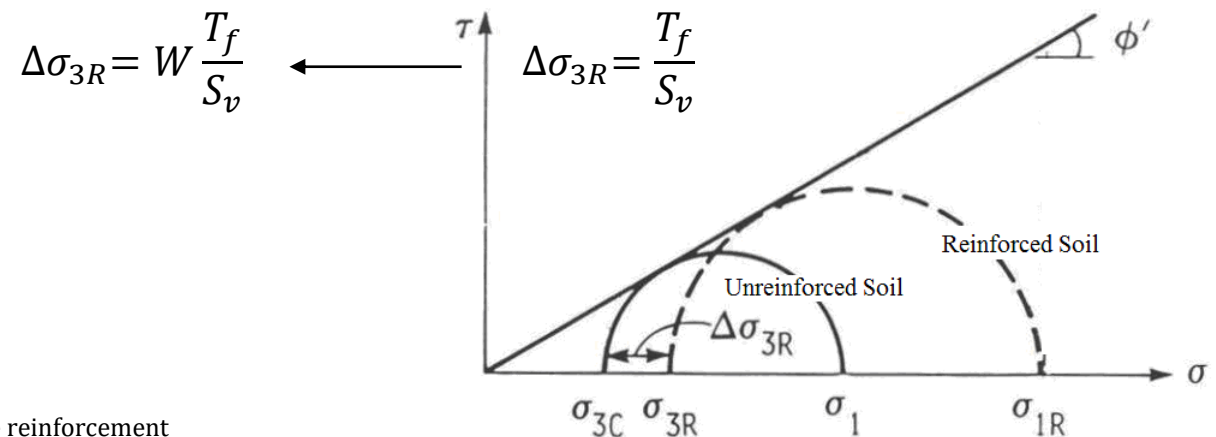
$$q_{ult,an} = \left[ \sigma_c + 0.7 \left( \frac{S_v}{6d_{max}} \right) \frac{T_f}{S_v} \right] K_{pr} + 2c\sqrt{K_{pr}}$$

$$K_{pr} = \tan^2 \left( 45 + \frac{\Phi_r}{2} \right)$$

Where  $q_{ult,an}$  is the ultimate capacity,  $\sigma_c$  is the external confining pressure caused by the facing,  $S_v$  is the reinforcement spacing,  $d_{max}$  is the maximum aggregate size,  $T_f$  is the tensile strength of reinforcement,  $\Phi_r$  is the internal friction angle of the reinforced backfill,  $c$  is the cohesion of the backfill,  $\gamma_b$  is the unit weight of facing block,  $\delta$  is the interface friction angle between geosynthetic and the facing block,  $d$  is the depth of the facing block unit, and  $K_{pr}$  is the coefficient of passive earth pressure



Introduction of apparent cohesion due to reinforcement (Pham, 2009)



Increase in axial strength and confinement pressure (Pham, 2009)

# Task 1: Review previous studies on GRS, design methods, material, and construction practices

- B: Deformations

- Lateral Displacement,  $D_L$

- Horizontal strain limited to 2%

FHWA-HRT-17-080 (2018)

- If vertical settlement is known

- $D_L = \frac{2b_{q,vol}D_v}{H}$       FHWA-HRT-11-026

Adams et al. (2012)

- $D_L = \frac{2b_{q,vol}D_v}{H} \times \frac{1}{n}$       NCHRP No. 24-41

Zornberg et al. (2018)

- If vertical settlement is unknown

- $D_L = \frac{\delta_R H}{75}$       for extensible reinforcement

FHWA Method

- $D_L = \left( \frac{\delta_R H}{50 \frac{J}{S_v} \frac{1}{p_o}} \right) \times \left( 1 + 1.25 \frac{q}{p_o} \right)$

Zornberg et al. (2018)

$$\delta_R = 11.81 \left( \frac{L}{H} \right)^4 - 42.25 \left( \frac{L}{H} \right)^3 + 57.16 \left( \frac{L}{H} \right)^2 - 35.45 \left( \frac{L}{H} \right) + 9.471$$

Where  $\delta_R$  is an empirically derived relative displacement coefficient (dimensionless),  $J$  is the reinforcement tensile stiffness defined by the secant modulus at 2% strain,  $L$  is the reinforcement length,  $q$  is the surcharge magnitude, and  $p_o$  is the atmospheric pressure.

# Task 1: Review previous studies on GRS, design methods, material, and construction practices

- C: Reinforcement Strength

- $T_{req} = \left( \frac{\sigma_h - \sigma_c - 2c\sqrt{K_{ar}}}{0.7\left(\frac{S_v}{6d_{max}}\right)} \right) S_v$

Pham (2009)

- $T_{req,i} = \begin{cases} \frac{1}{2} K_{ar} \gamma H S_v + \Delta\sigma_H S_v & \text{for } S_v \geq 16'' \\ \frac{1}{2} K_{ar} \gamma H S_v + \Delta\sigma_H S_v & \text{for } S_v \leq 8'' \\ K_{ar} \gamma S_v \left[ z_i + \left( \frac{16'' - S_v}{8''} \right) \left( \frac{H}{2} - z_i \right) \right] + \Delta\sigma_H S_v & \text{for } 8'' \leq S_v \leq 16'' \end{cases}$

Zornberg et al. (2018)

Where  $K_{ar}$  is the active earth pressure coefficient,  $\gamma$  is the backfill total unit weight,  $H$  is the total height of GRS composite,  $z_i$  is the depth of backfill at position  $i$ , and  $\Delta\sigma_H$  is the change in the horizontal earth pressure of the backfill due to the applied surcharge.

## Task 2: Design experimental plan for performance tests

Test No	Backfill					Reinforcement				
	Type	Maximum Dry Unit weight (pcf)	Compacted to Dry Unit weight (pcf)	Peak Friction angle (degrees)	Cohesion (psi)	Type	Ultimate Tensile Strength, $T_f$ (lb/ft) (MD X CD)	$S_v$ (inch)	B (ft)	H/B
<b>PT-01</b>	#57 stone	96.2	96.85	44.08	0	Mirafi HP570	4,800 x 4,800	8	3	2
<b>PT-02</b>	#57 stone	96.2	97.59	44.08	0	Mirafi HP770	7,200 x 5,760	8	3	2
<b>PT-03</b>	#57 stone	96.2	96.55	44.08	0	TerraTex HPG57	4,800 x 4,800	8	3	2
<b>PT-04</b>	RCA-GAB	115.9	113.28	58.41	2.87	Mirafi HP570	4,800 x 4,800	8	3	2
<b>PT-05</b>	RCA-GAB	115.9	113.70	58.41	2.87	Mirafi HP770	7,200 x 5,760	8	3	2
<b>PT-06</b>	RCA-GAB	115.9	113.94	58.41	2.87	TerraTex HPG57	4,800 x 4,800	8	3	2
<b>PT-07</b>	FGA	16.75	18.20	54.0 <sup>b</sup>	1.28 <sup>b</sup>	Mirafi HP770	7,200 x 5,760	8	3	2
<b>PT-08**</b>	#57 stone	96.2	97.00	44.08	0	Mirafi HP570	4,800 x 4,800	8	3	2

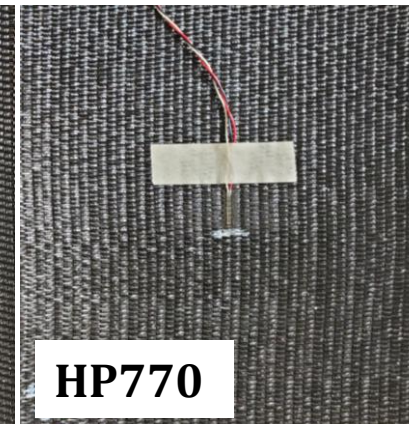
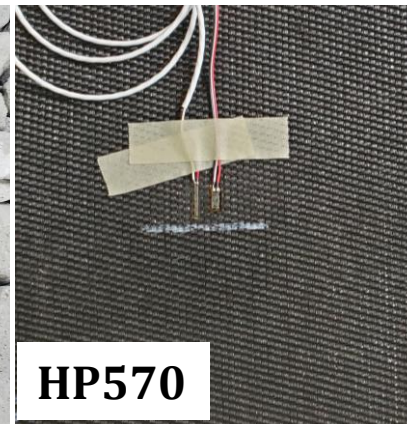
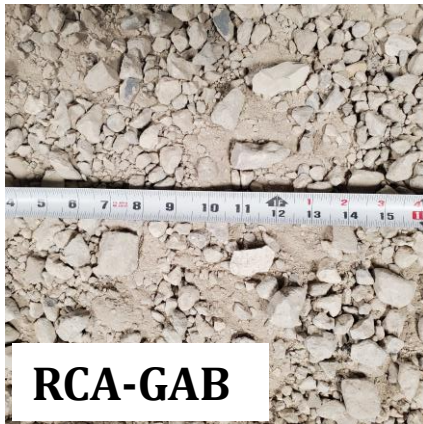
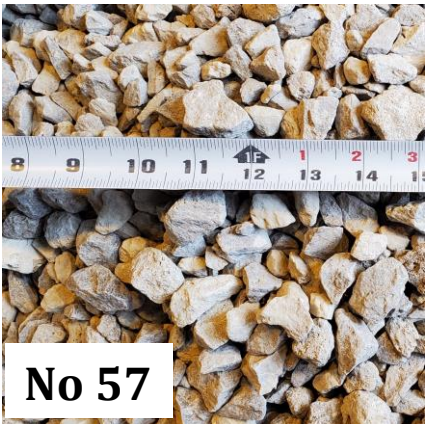
\*\* Block cells in the upper three courses of blocks contain concrete and rebar, <sup>b</sup> based on a 12 in x 12 in direct shear box.

## Task 2: Design experimental plan for performance tests

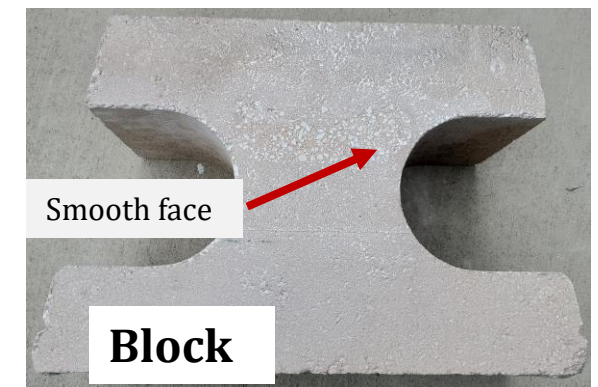
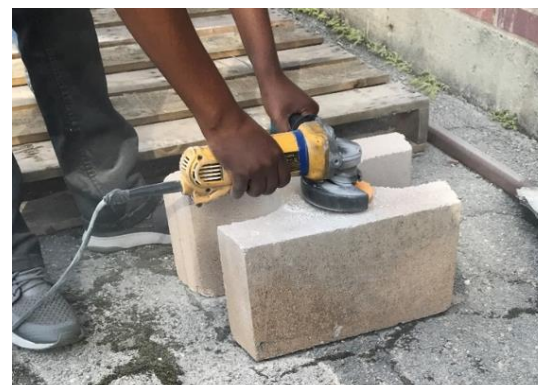
- Materials

### Aggregates

### Geotextile

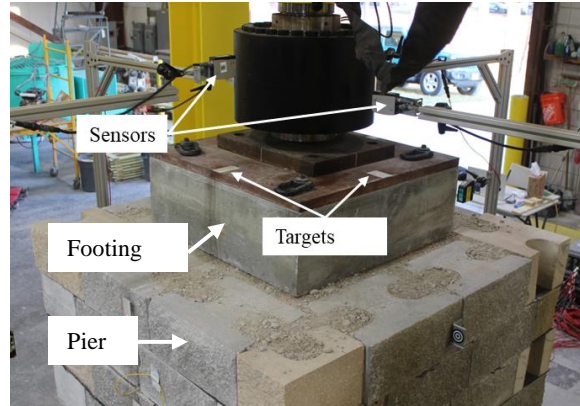


### Facing blocks

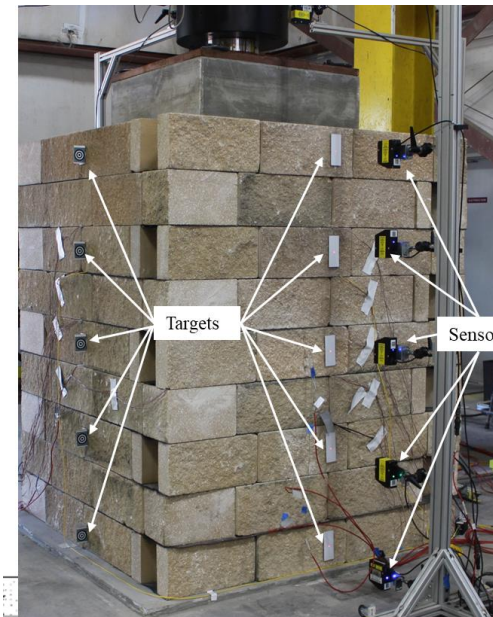


## Task 2: Design experimental plan for performance tests

- Displacement
  - Vertical: Four at top of footing
  - Lateral: Five on each wall
- Reinforcement strain
  - Strain gauge: First test
  - Fiber optic strain sensor
  - Five geotextiles instrumented
- Earth pressure
  - Vertical: At the bottom
  - Lateral : At the middle of the pier
- Applied load
  - Load cell



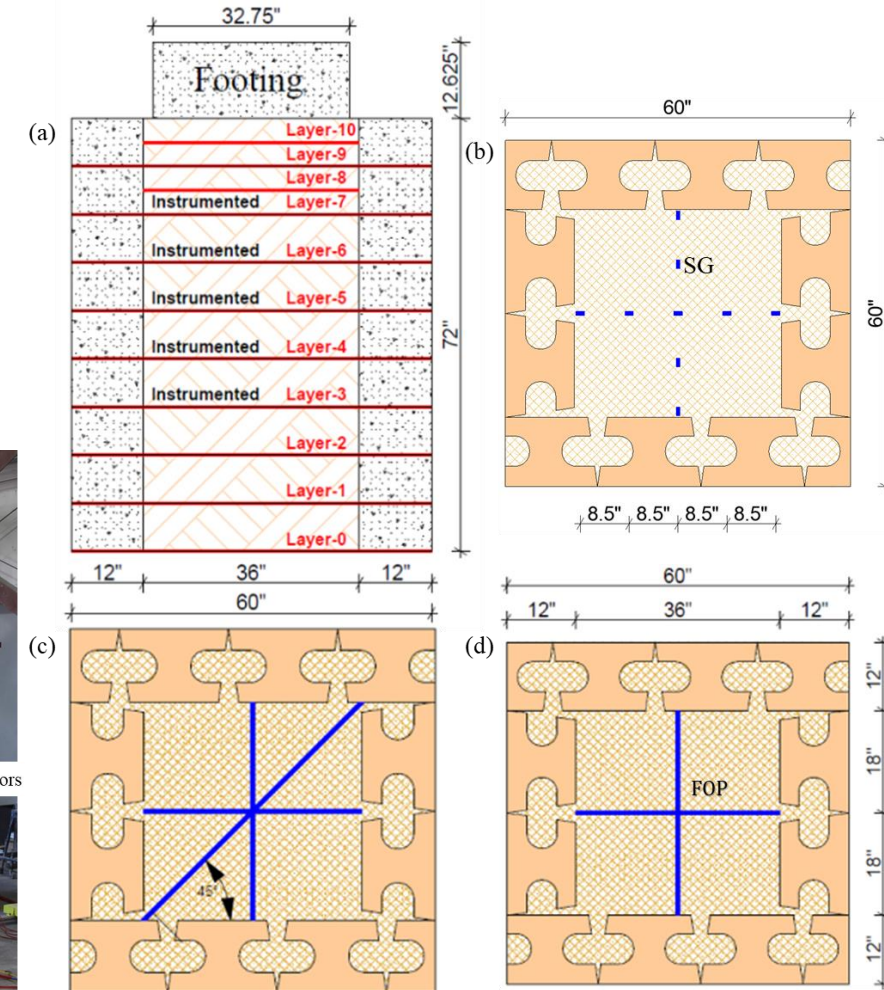
Vertical displacement measurement



Lateral displacement measurement



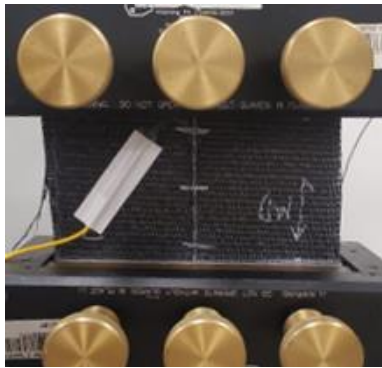
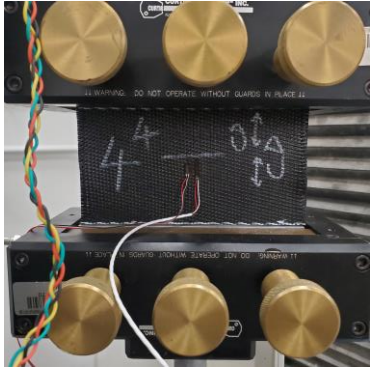
Vertical earth pressure cell



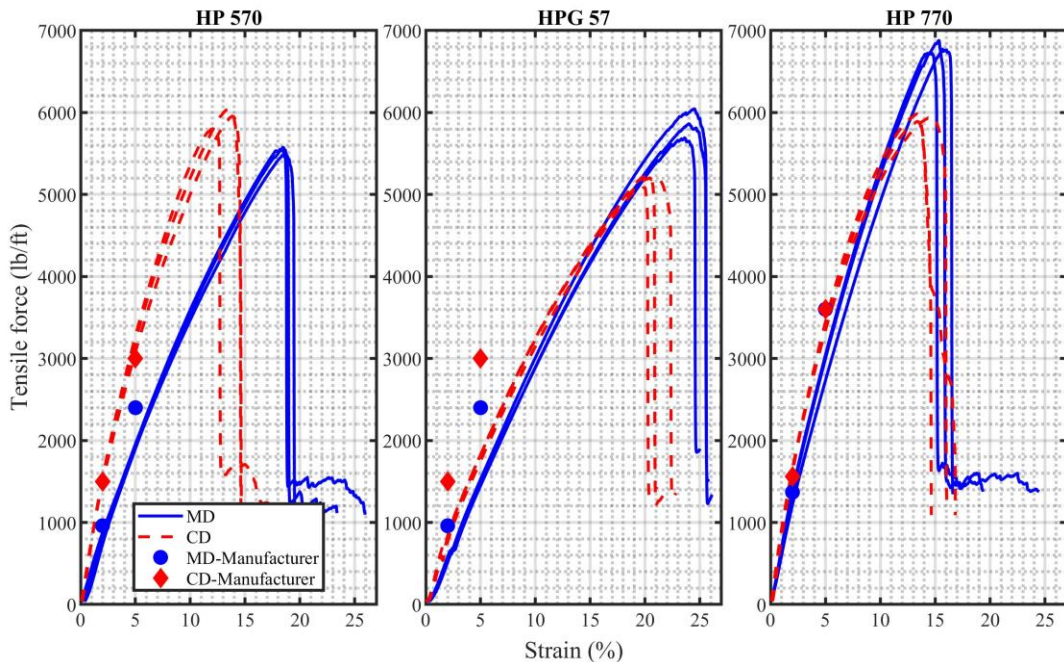
Installation of strain gauges and fiber optic strain sensor  
SG: Strain Gauge; FOP: Fiber optic cable

# Task 2: Design experimental plan for performance tests

- Geotextile

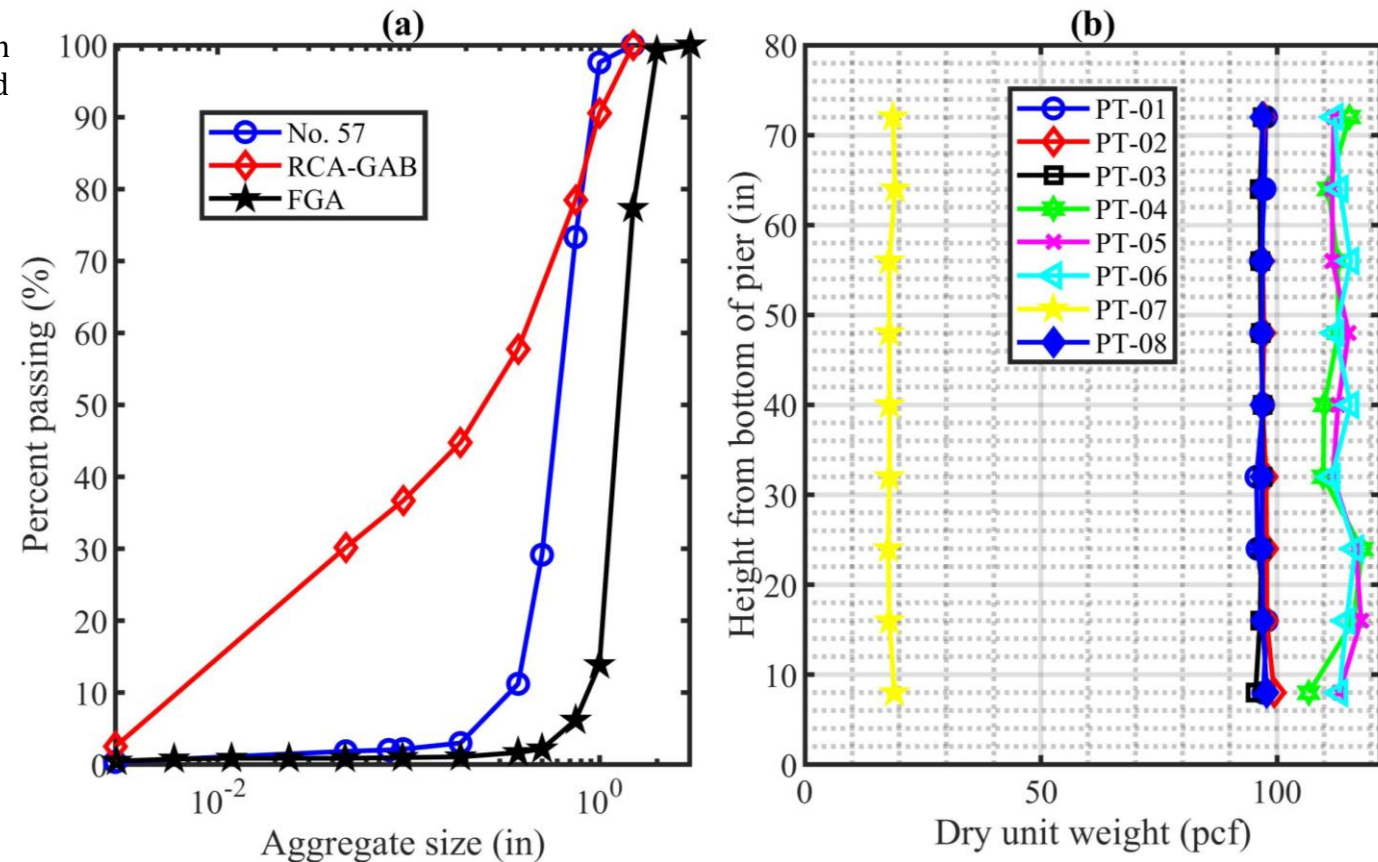


Uniaxial tensile tests of geotextile: Test specimen with strain gauges installed; and Test specimen with fiber strain sensor installed



Tensile strength results

- Aggregates



(a) Sieve analysis results; (b) Dry unit weight during construction

# Task 2: Design experimental plan for performance tests

- Aggregates

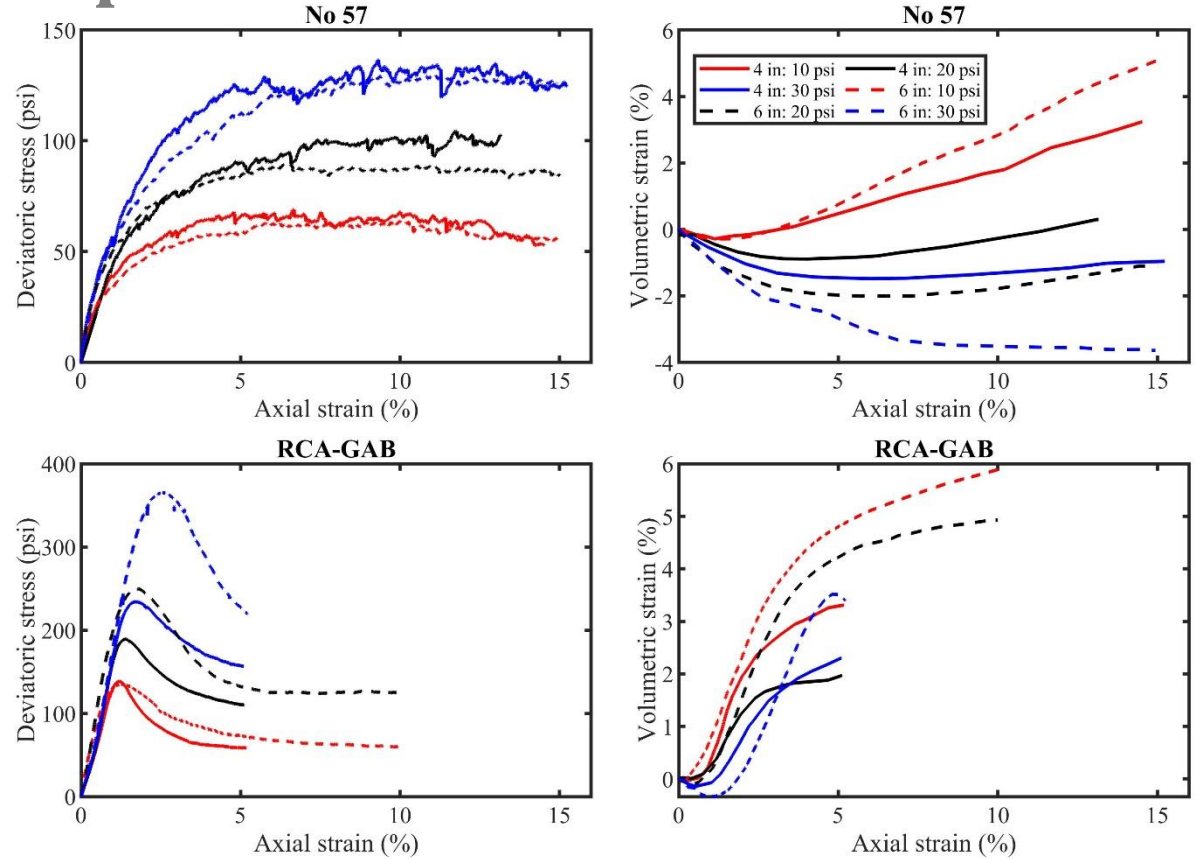


6" diameter triaxial test

Strength properties at peak

Aggregate type	Peak	
	Friction angle (°)	Apparent Cohesion (psi)
No. 57 4-inch specimen	45.21	0
No. 57 6-inch specimen	44.08	0
RCA-GAB 4-inch specimen	47.03	14.91
RCA-GAB 6-inch specimen	58.41	2.87

Triaxial results from 4- and 6-inch specimen



Interface properties between Geotextile and Backfill

Geotextile	Interface friction angle (°)	
	No 57	RCA-GAB
HP570	42.23	40.39
HPG57	37.95	38.35
HP770	37.66	37.33

Interface properties between Geotextile and blocks

Geotextile	Interface Friction angle (°)
HP570	21.86
HPG57	22.75
HP770	21.84

# Task 2: Design experimental plan for performance tests

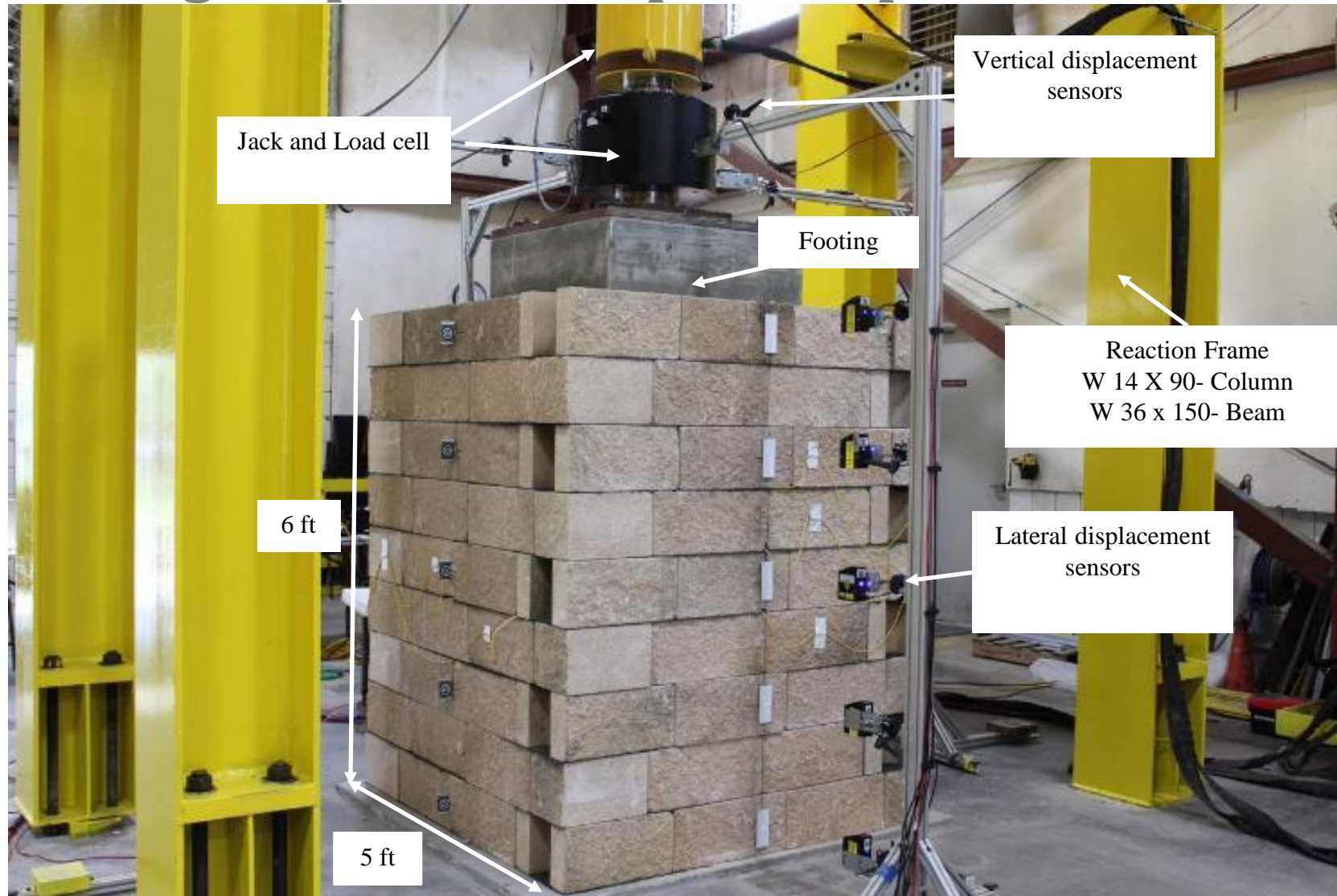
- Bottom-Up pier construction
  - Laying facing blocks
  - Placing and compacting backfill
  - Laying down geosynthetics



(a) Laying the face blocks, (b and c) Placing and compacting backfill, (d) Laying down geosynthetics, (e, f, and g) Repeat A-C to achieve final height

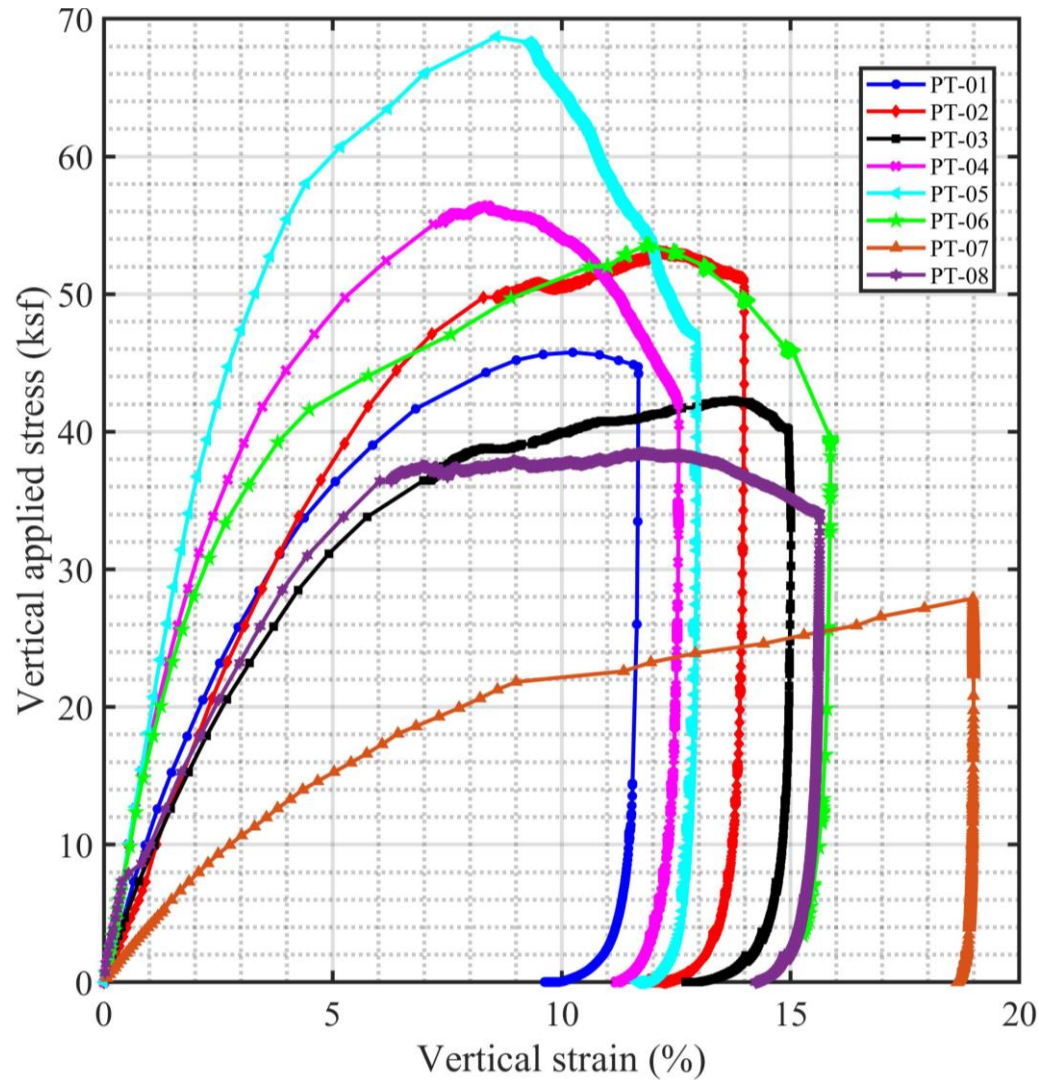


## Task 2: Design experimental plan for performance tests

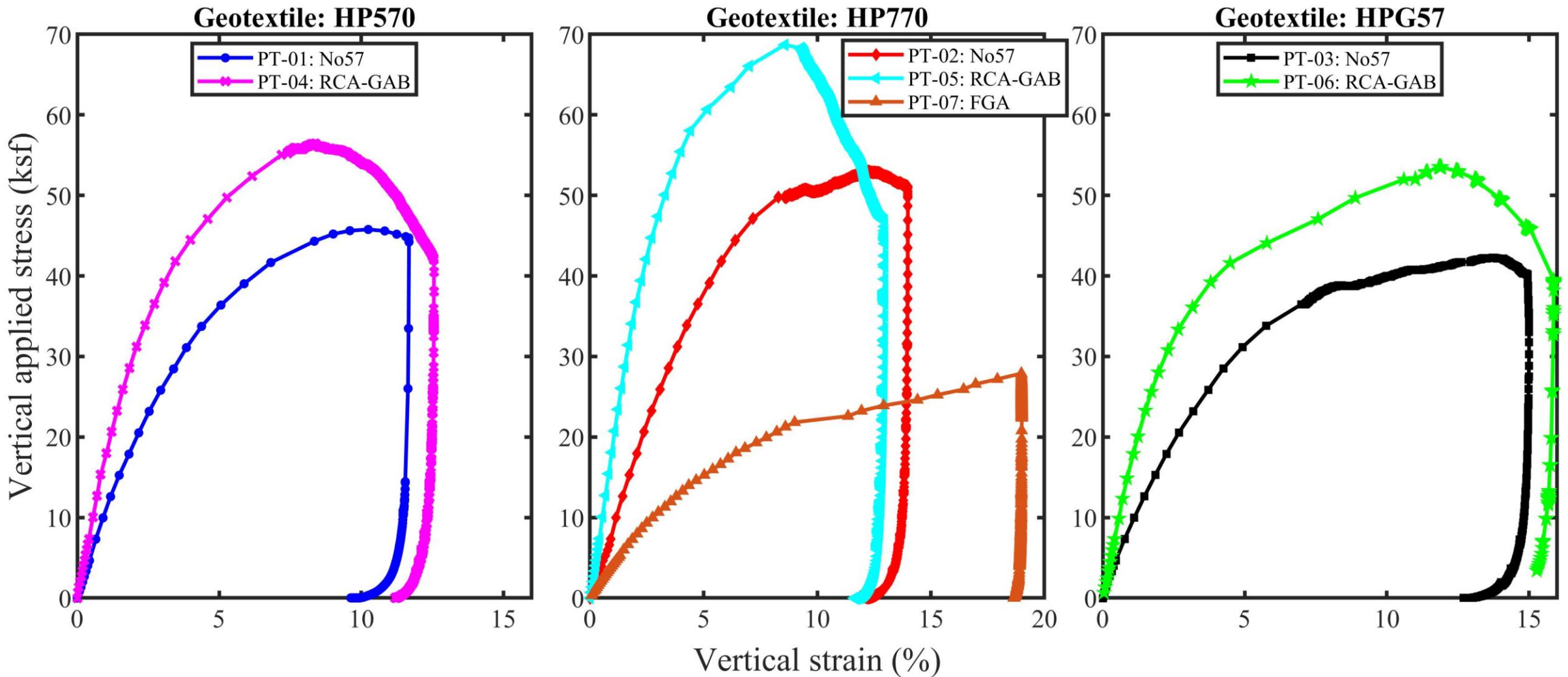


Completed and instrumented pier before testing PT-01

## Task 3: Performance tests – axial load-deformation tests on GRS



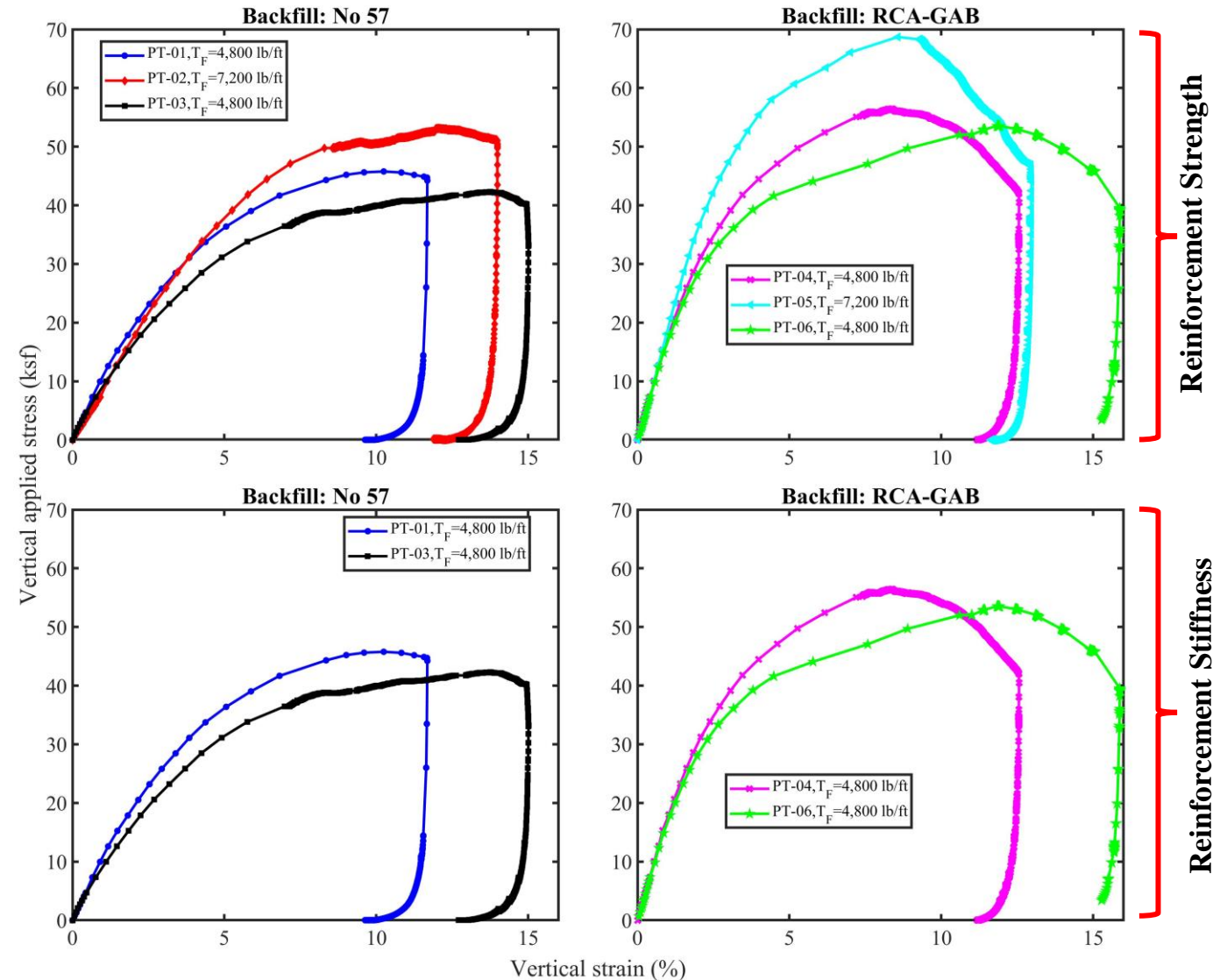
# Task 3: Performance tests – axial load-deformation tests on GRS



A plot of applied vertical stress versus average vertical strain

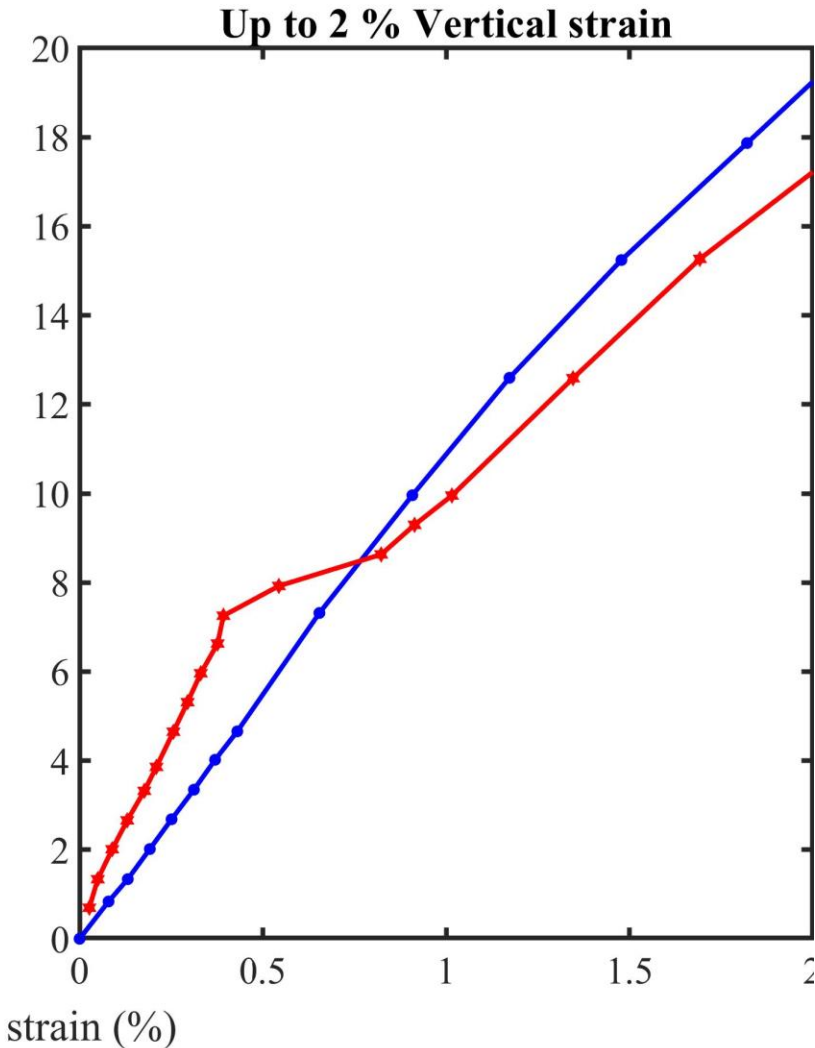
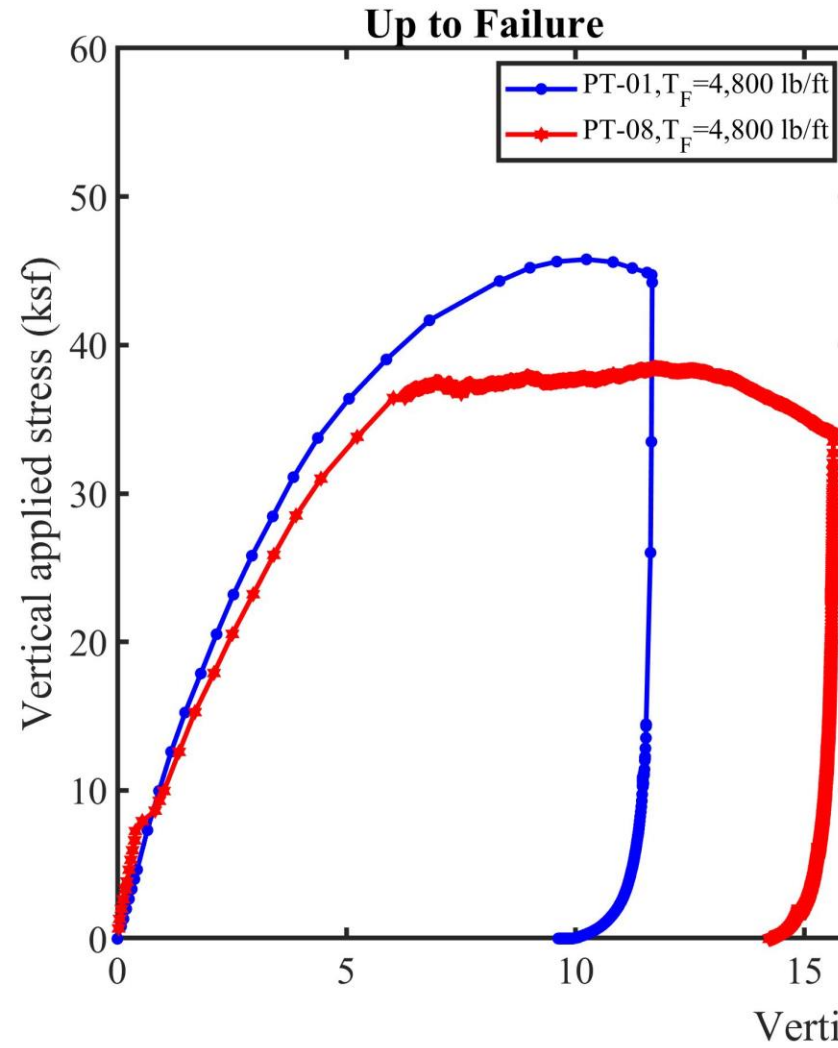
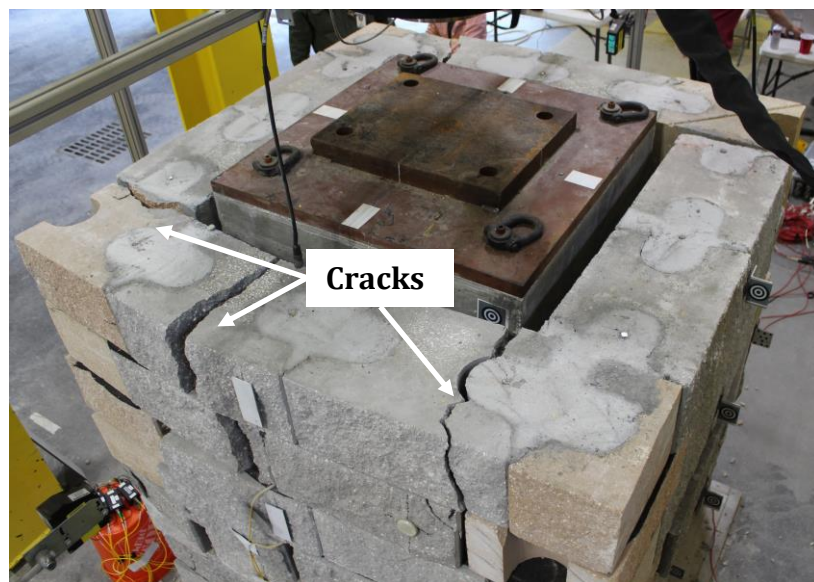
## Task 3: Performance tests - reinforcement strength and stiffness

- Higher reinforcement strength
  - Higher vertical capacity
- Higher reinforcement stiffness
  - Stiffer load response



## Task 3: Performance tests - concrete fill

- Concrete fill
  - Increases initial stiffness of the global stress-strain up to 7.25 ksf
  - Reduces the vertical capacity slightly
  - More cracks on blocks



A plot of applied vertical stress versus average vertical strain

# Task 3: Performance tests - lateral displacement

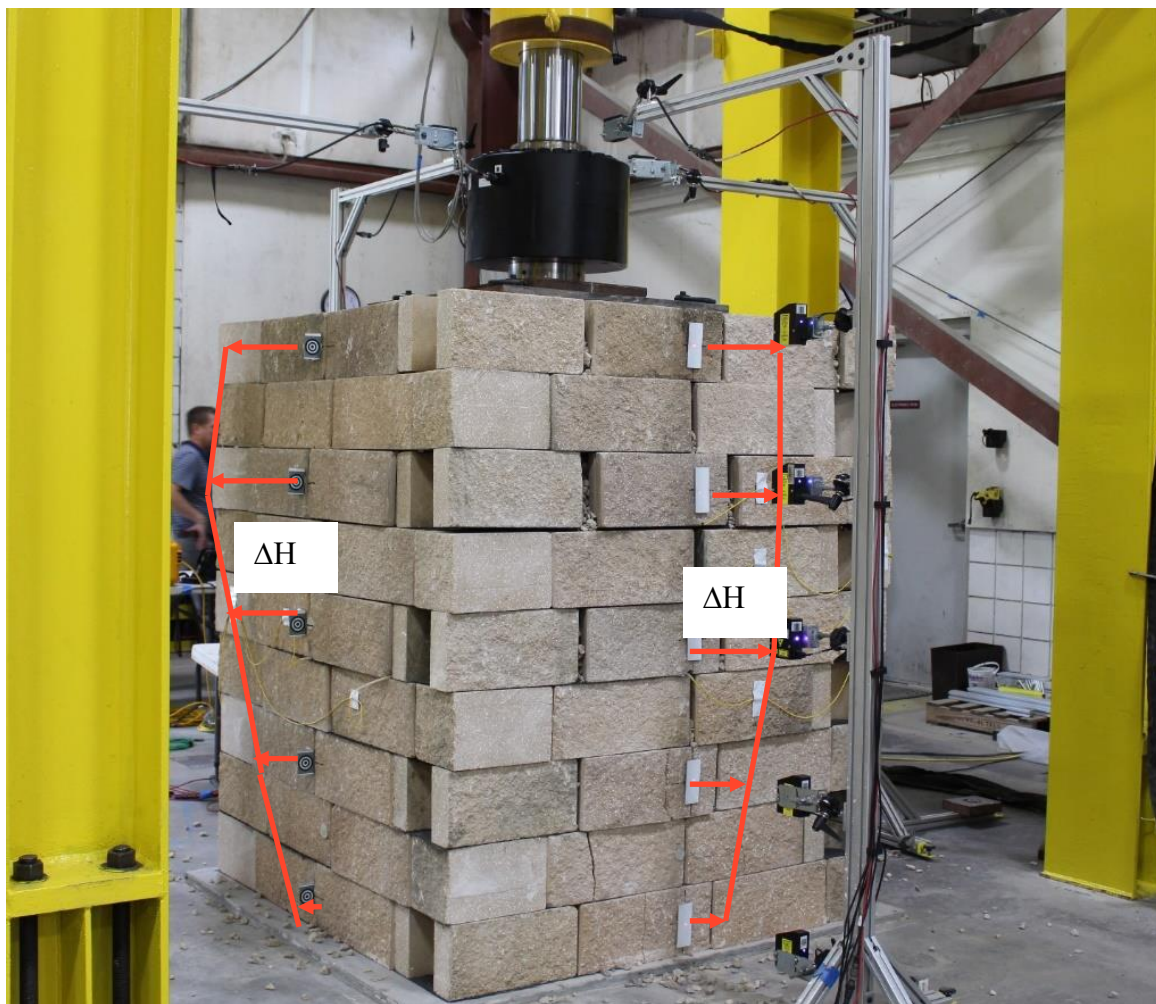
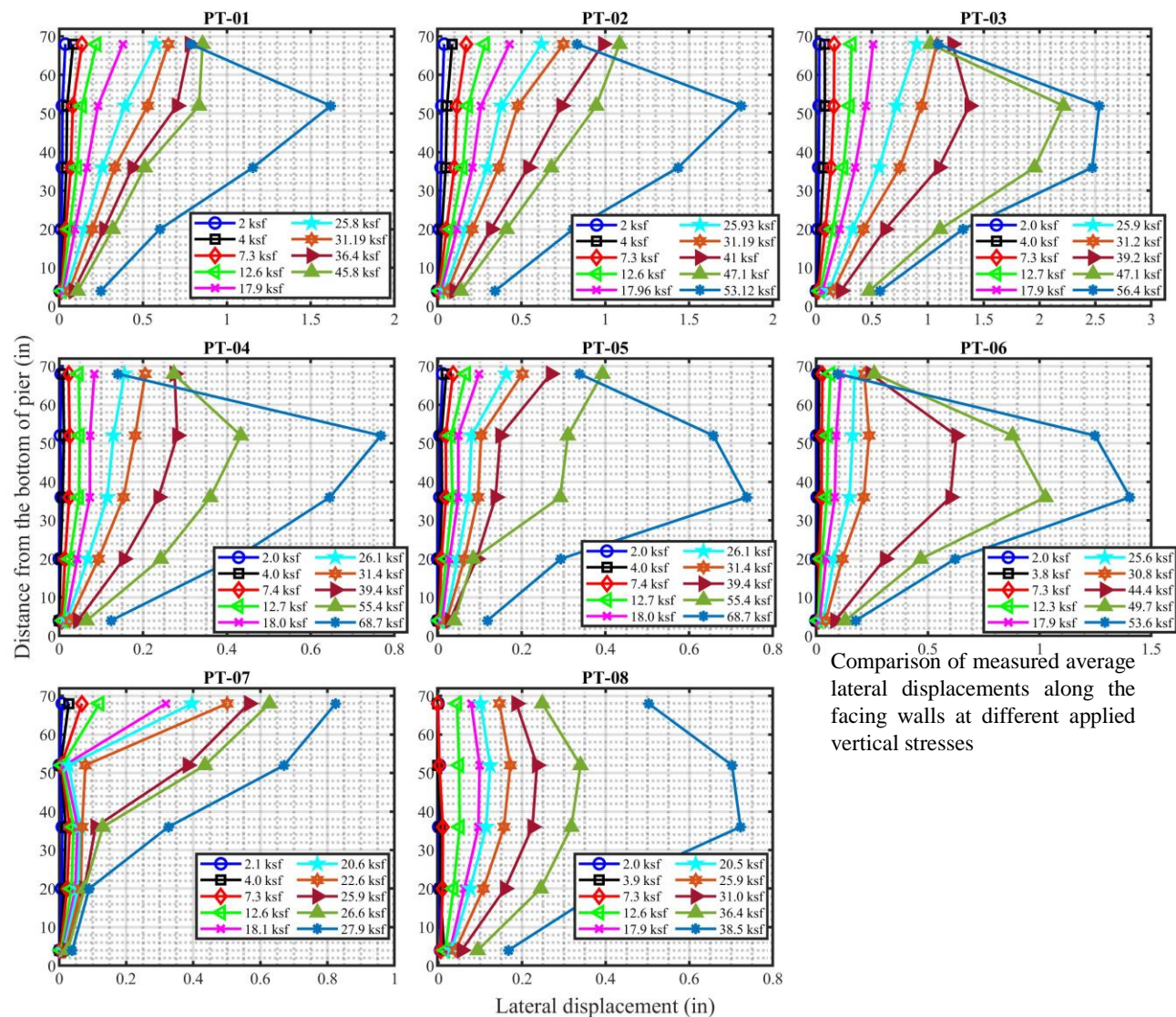
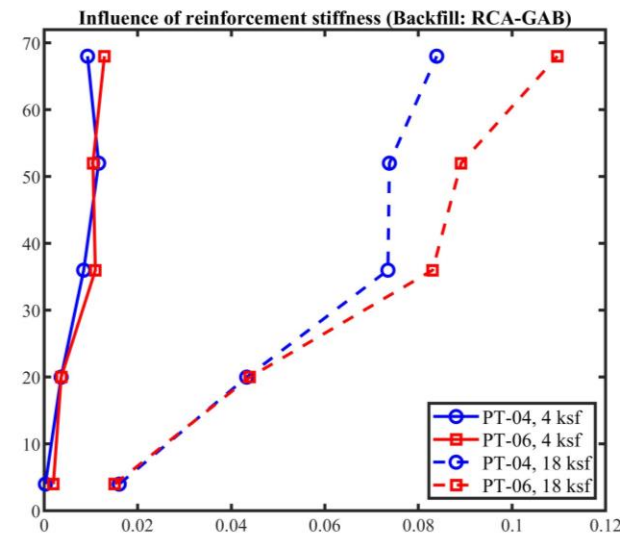
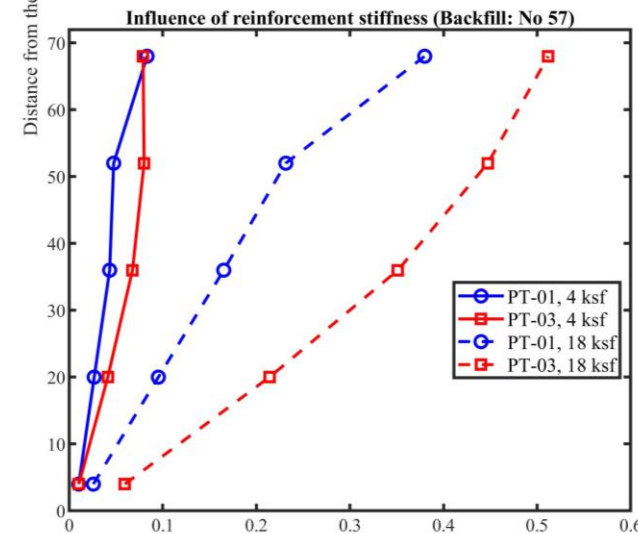
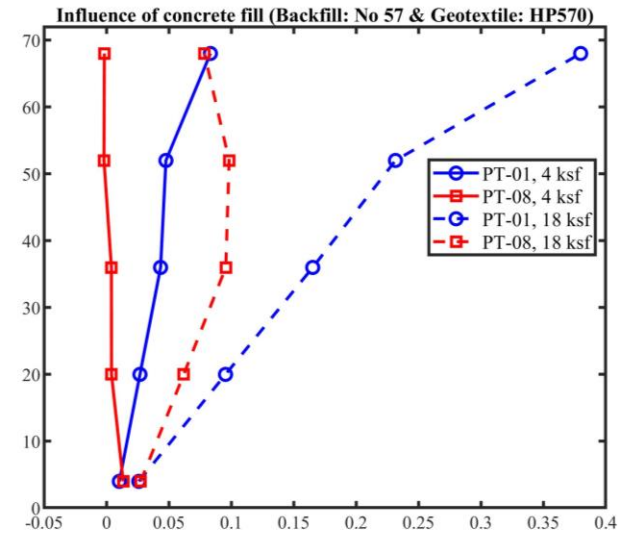
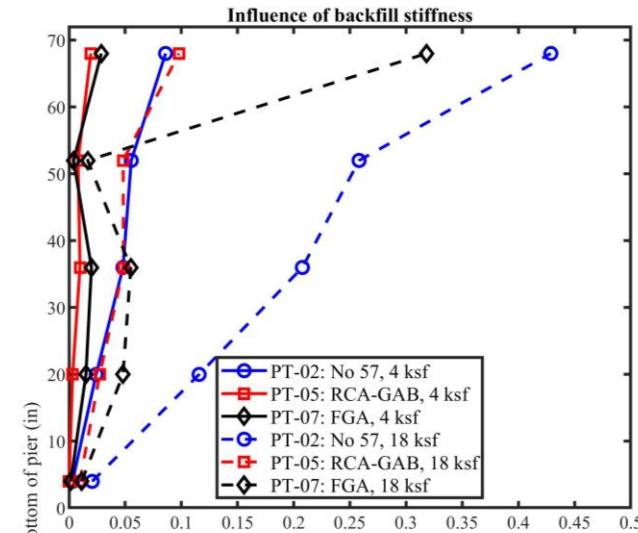


Illustration of lateral displacement after the test



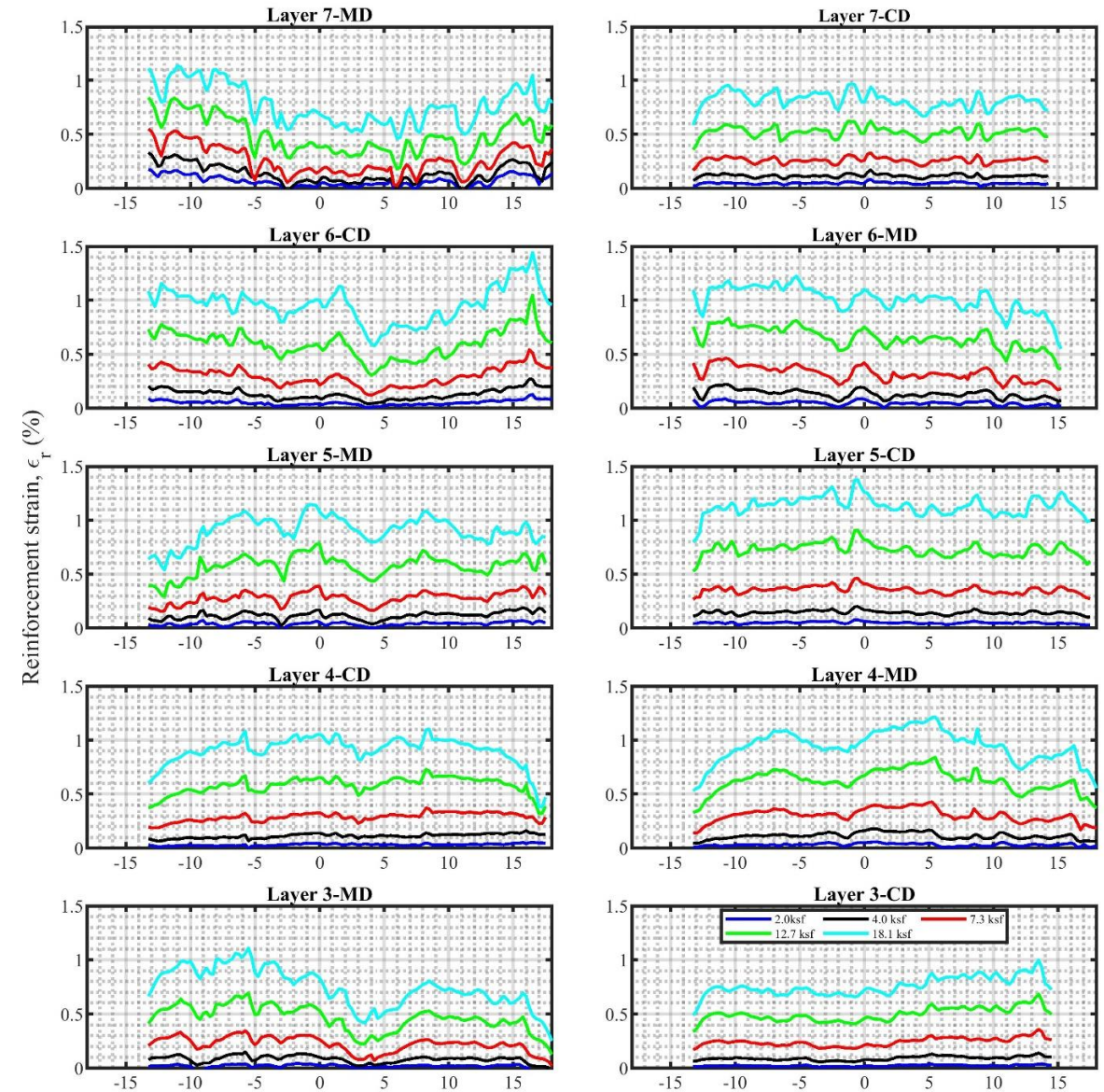
## Task 3: Performance tests - lateral displacement

- Higher stiffness of backfill
  - Lower lateral displacement
- Lower geotextile stiffness (HPG 57)
  - Larger lateral displacement
- Concrete fill (in PT-08)
  - Reduces lateral displacement
  - Changes lateral displacement profile
- Higher compressibility (FGA backfill)
  - Changes the displacement profile
  - Less displacement at the seventh block layer at smaller applied vertical stress
  - More compression at the top layer



## Task 3: Performance tests - reinforcement strain

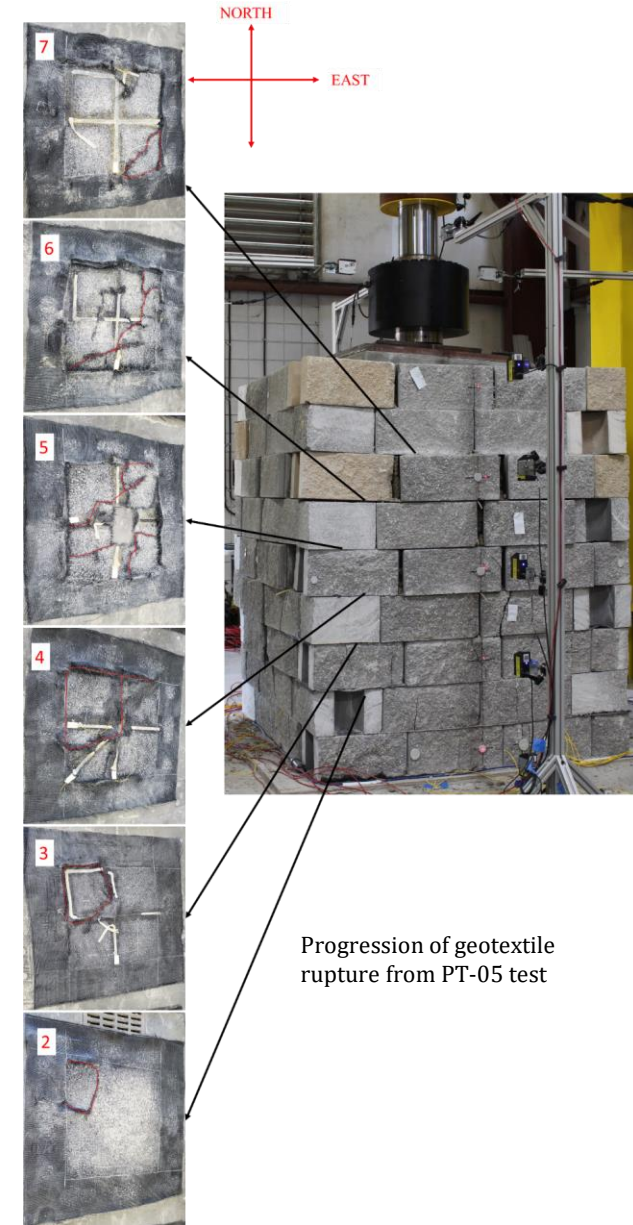
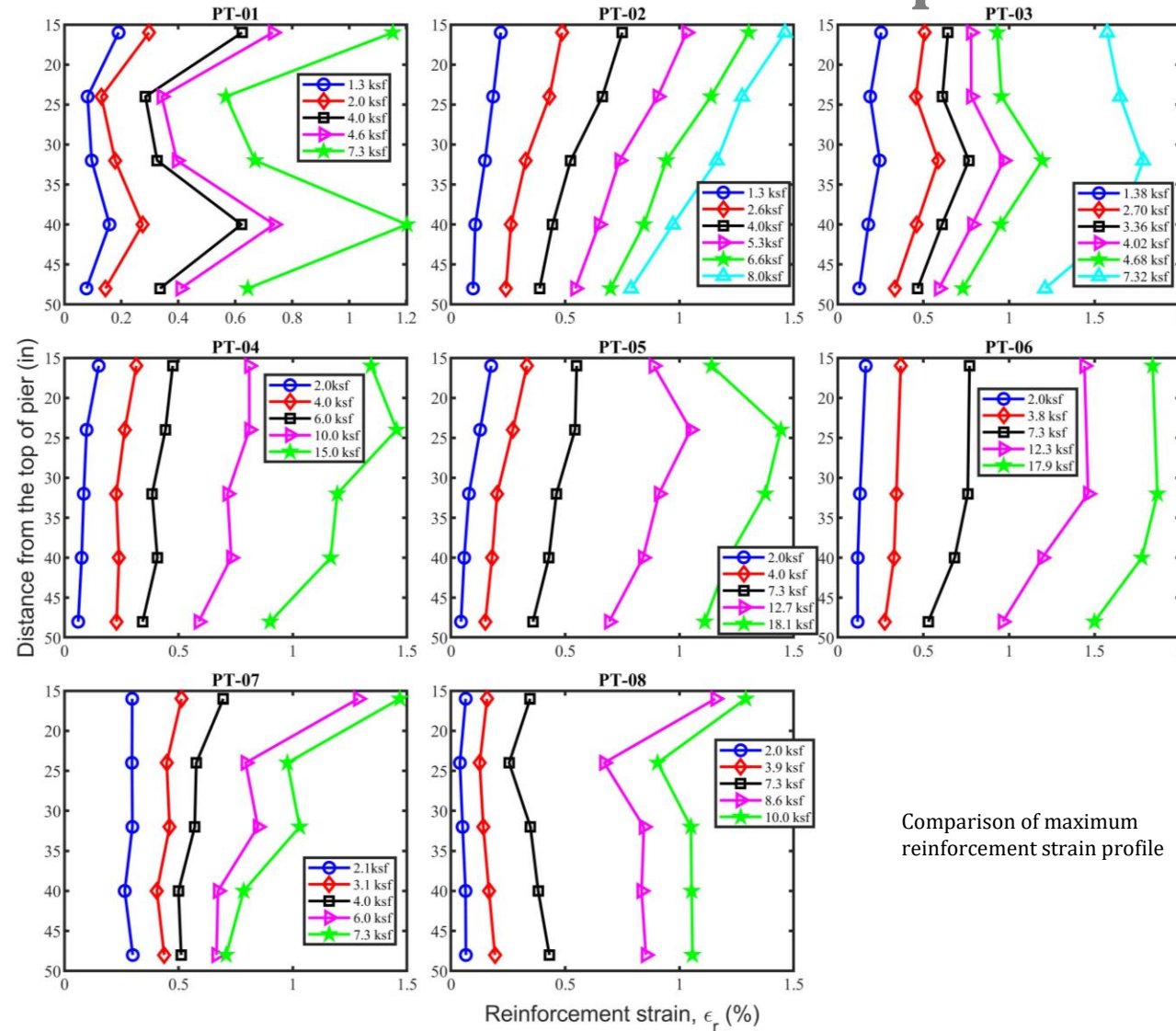
- Tensile strain  $\uparrow$  Applied load  $\uparrow$
- Upper layers (Layer 6 & 7)
  - Tensile strains were the greatest near the facing blocks
- Layer 4 & 5
  - Maximum strains were around the center of the geotextile within the soil mass
- Backfill stiffness
  - Affects the magnitude of tensile strain
  - Doesn't affect the nature of strain distribution



Reinforcement strain distribution in geotextile at different applied vertical stress for PT-05

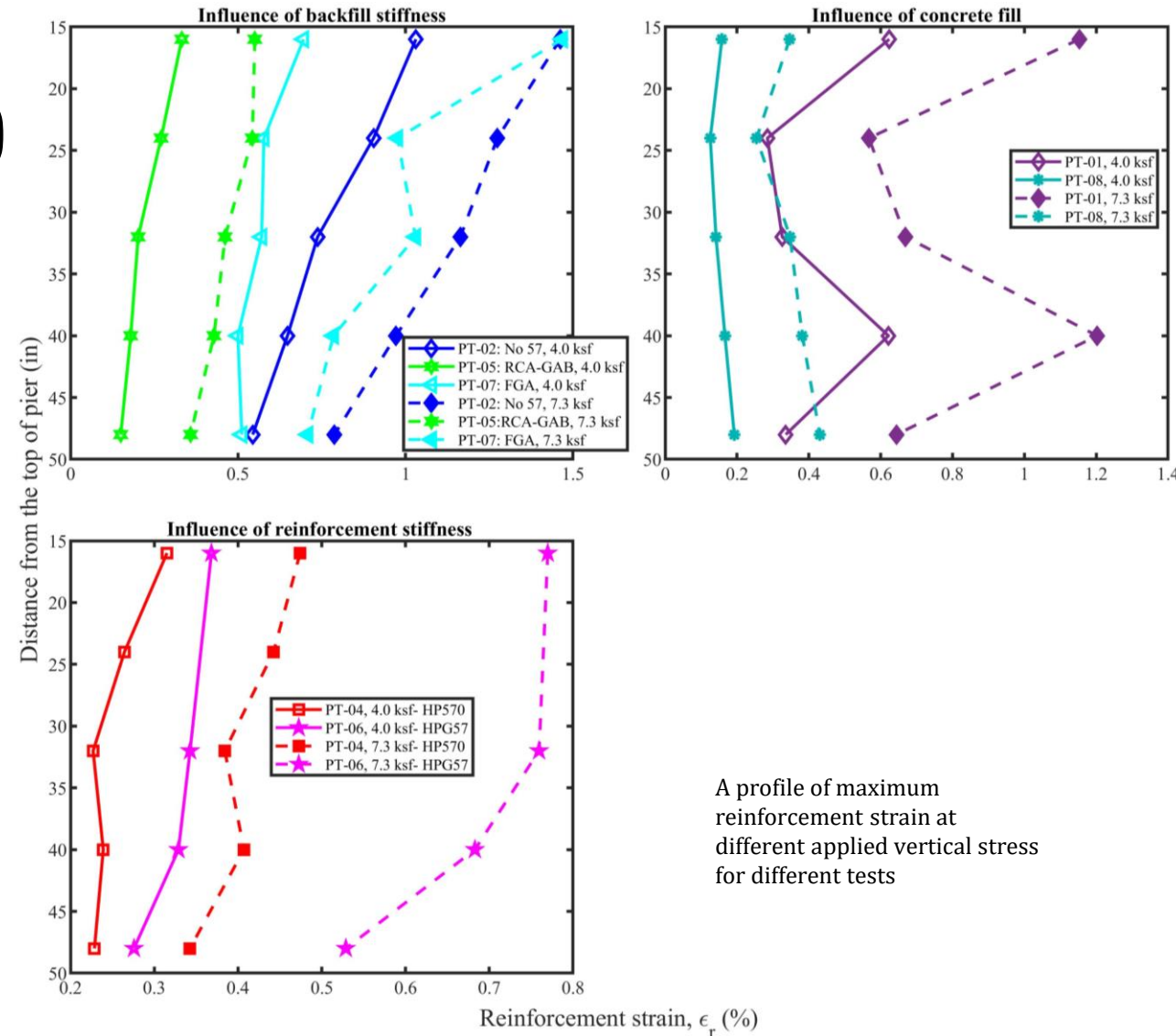
# Task 3: Performance tests – tension strain profile

- Maximum reinforcement strain
  - Within the top half of the pier height
  - Initially appears at the seventh layer for lower vertical stresses but shifts to the sixth or fifth layer as more load is applied



## Task 3: Performance tests - reinforcement strain profile

- Higher backfill stiffness (RCA-GAB)
  - Small reinforcement strain
- Lower backfill stiffness (No 57 & FGA)
  - Greater reinforcement strain
- Higher reinforcement stiffness
  - Lower reinforcement strain
- Concrete fill (in PT-08)
  - Reduces reinforcement strains
  - Reduces the reinforcement strain at the top



# Task 4: Comparison with design methods: ultimate vertical capacity

## FHWA Method

$$q_{ult,an} = \left[ \sigma_c + 0.7 \left( \frac{S_v}{6d_{max}} \right) \frac{T_f}{S_v} \right] K_{pr} + 2c\sqrt{K_{pr}}$$

$$K_{pr} = \tan^2 \left( 45 + \frac{\Phi_r}{2} \right)$$

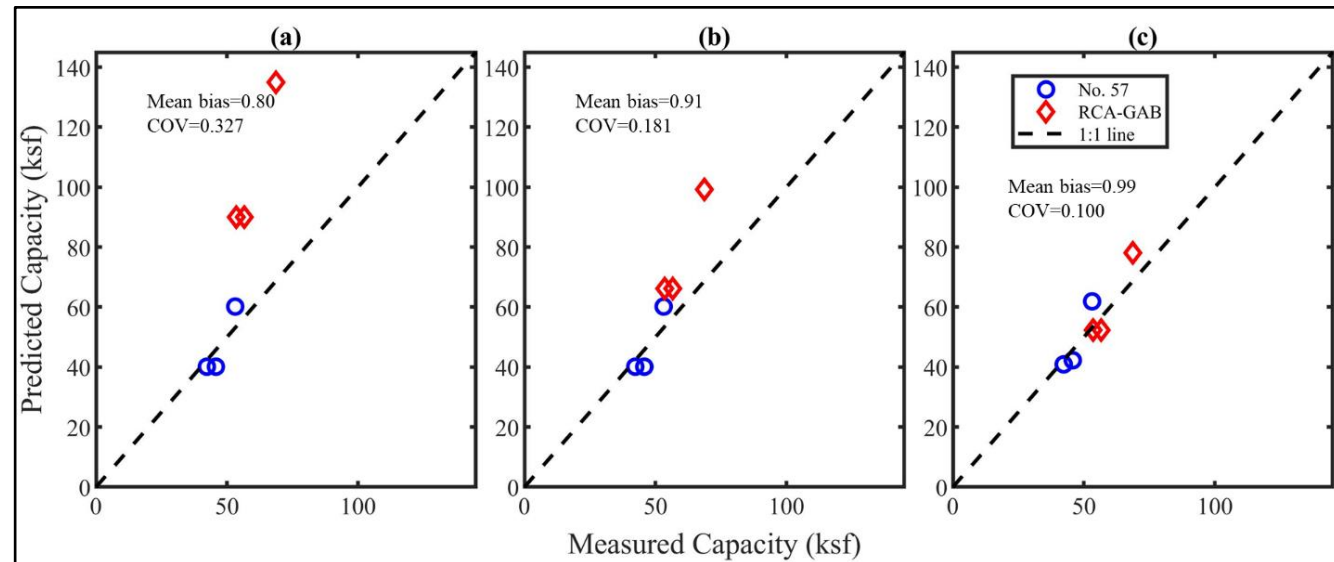
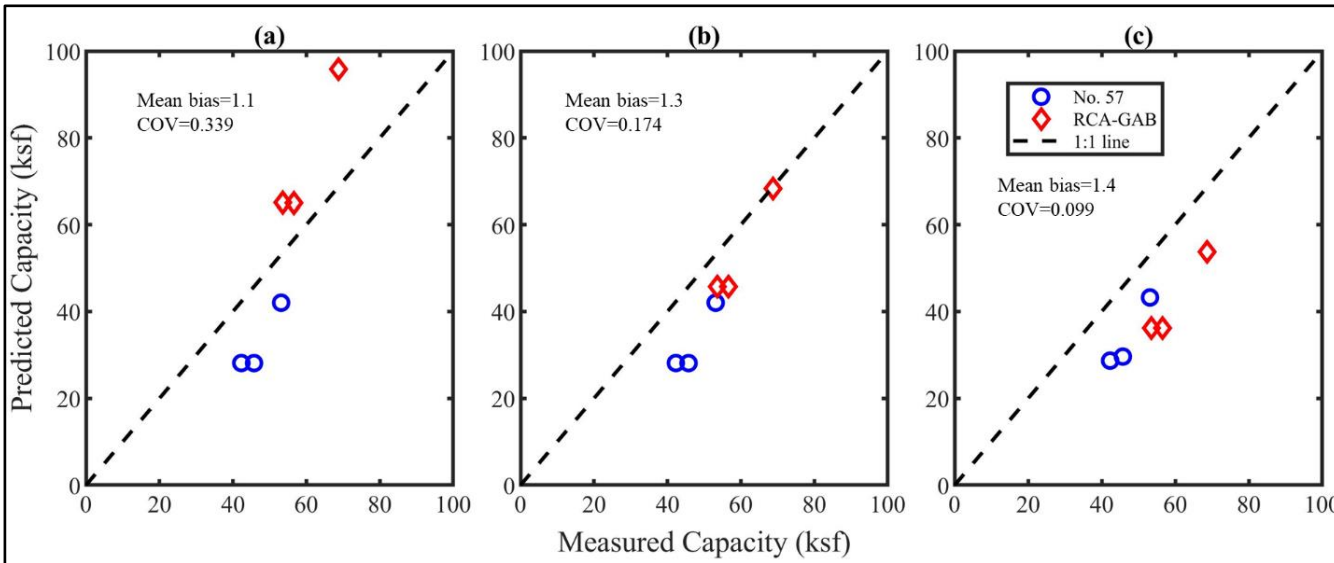
Where  $q_{ult,an}$  is the ultimate capacity,  $\sigma_c$  is the external confining pressure caused by the facing,  $S_v$  is the reinforcement spacing,  $d_{max}$  is the maximum aggregate size,  $T_f$  is the tensile strength of reinforcement,  $\Phi_r$  is the internal friction angle of the reinforced backfill,  $c$  is the cohesion of the backfill,  $\gamma_b$  is the unit weight of facing block,  $\delta$  is the interface friction angle between geosynthetic and the facing block,  $d$  is the depth of the facing block unit, and  $K_{pr}$  is the coefficient of passive earth pressure

← Comparison of the measured and predicted vertical capacities(FHWA Method).  
(a) Based on peak friction angle; (b) Based on residual friction angle; (c) Based on secant friction angle at failure of GRS pier. **Backfill strength parameters from a 6-in triaxial test were used in calculation**

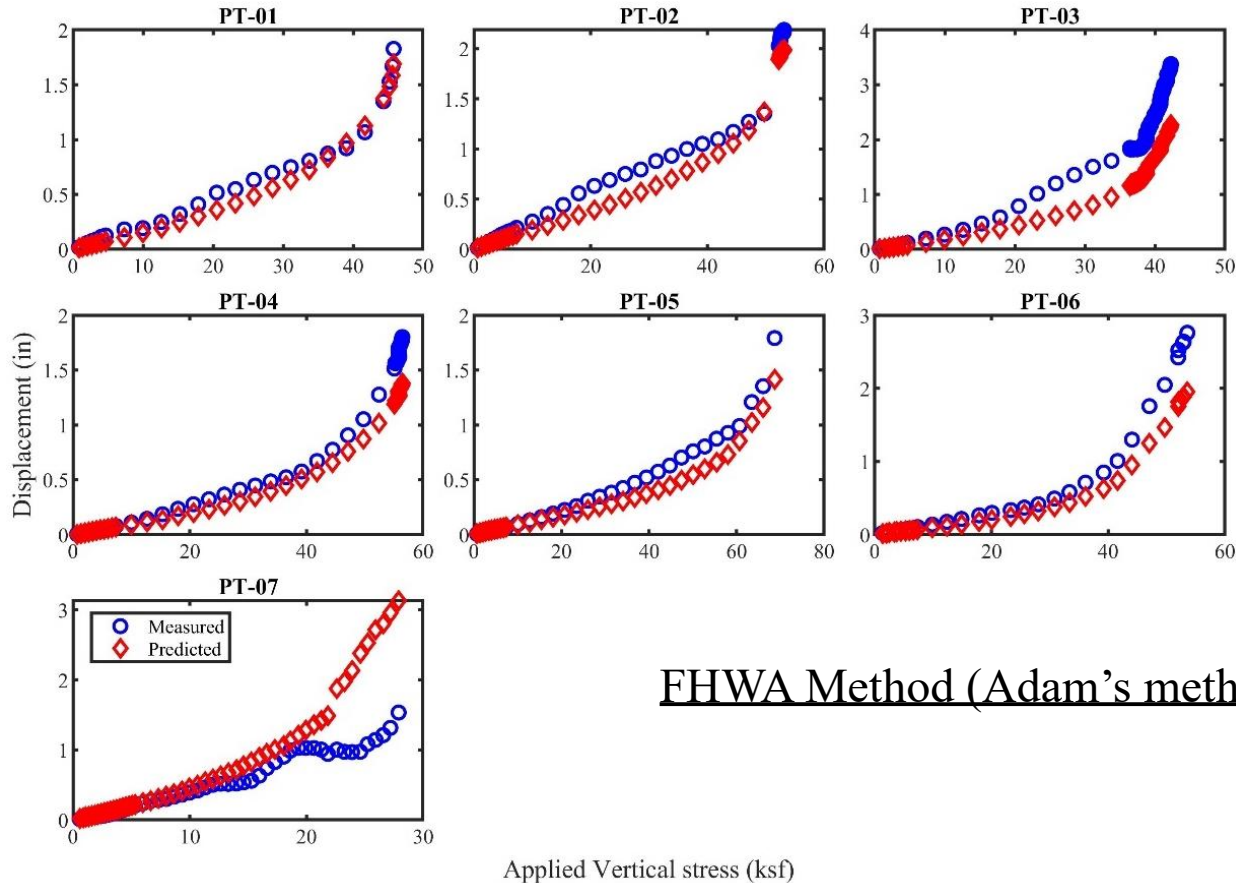
## Hoffman's Method

$$q_{ult,an} = \frac{T_f}{S_v} K_{pr}$$

← Comparison of the measured and predicted vertical capacities(Hoffman Method)  
(a) Based on peak friction angle; (b) Based on residual friction angle; (c) Based on secant friction angle at failure of GRS pier. **Backfill strength parameters from a 6-in triaxial test were used in calculation**



# Task 4: Comparison with design methods - Lateral Displacement



## FHWA Method (Adam's method)

A comparison of measured and predicted maximum lateral displacement during loading.

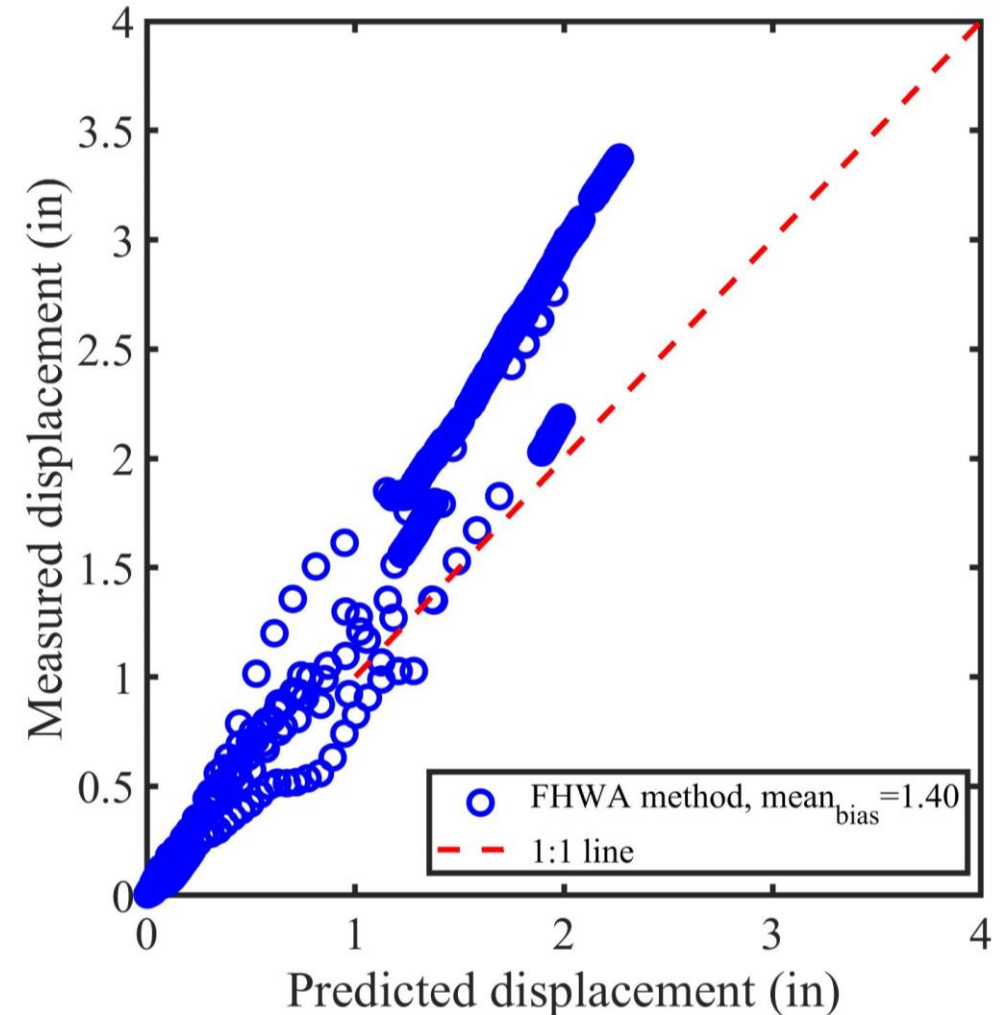
For abutment wall

$$D_L = \frac{2b_{q,vol}D_v}{H}$$

For pier walls

$$D_L = \frac{2b_{q,vol}D_v}{H} \times \frac{1}{4}$$

Where  $D_L$  is the maximum lateral deformation,  $D_v$  is the vertical settlement of GRS abutment,  $b_{q,vol}$  is the width of the load along the top of the wall, and  $H$  is the height of the abutment.



A comparison of measured and predicted maximum lateral displacement (With outlier removed from PT-07)

# Task 4: Comparison with design methods - vertical earth pressure

## 2:1 Approximate method

$$\Delta\sigma_z = \frac{Q_v}{D_1(L+z)}$$

$$D_1 = b_f + z, \text{ for } z \leq z_1$$

$$D_1 = \frac{b_f + z}{2} + d, \text{ for } z > z_1$$

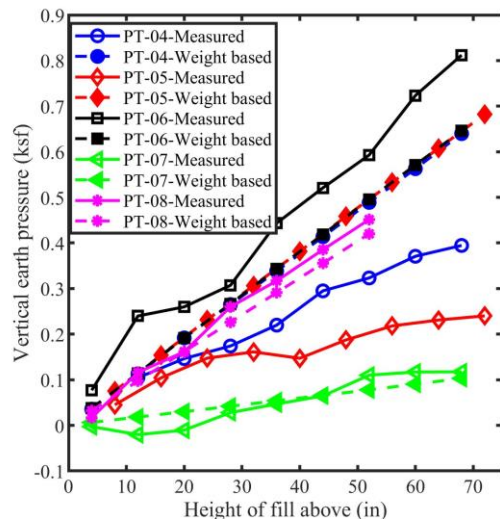
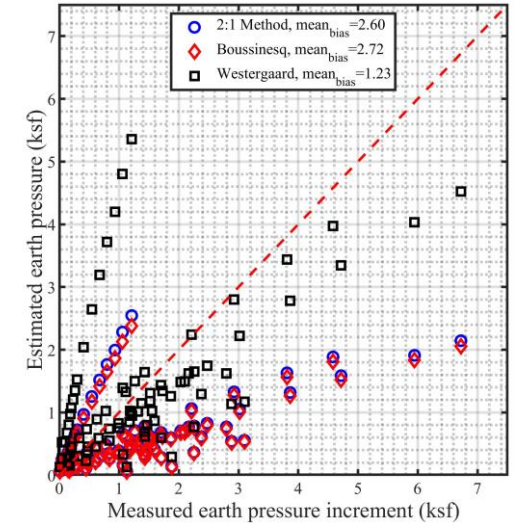
## Boussinesq theory

$$\Delta\sigma_z = \frac{q}{4\pi} \left[ \left( \frac{2mn(m^2 + n^2 + 1)^{0.5}}{(m^2 + n^2 + m^2n^2 + 1)} \right) \left( \frac{m^2 + n^2 + 2}{m^2 + n^2 + 1} \right) + \tan^{-1} \left( \frac{2mn(m^2 + n^2 + 1)^{0.5}}{m^2 + n^2 - m^2n^2 + 1} \right) \right]$$

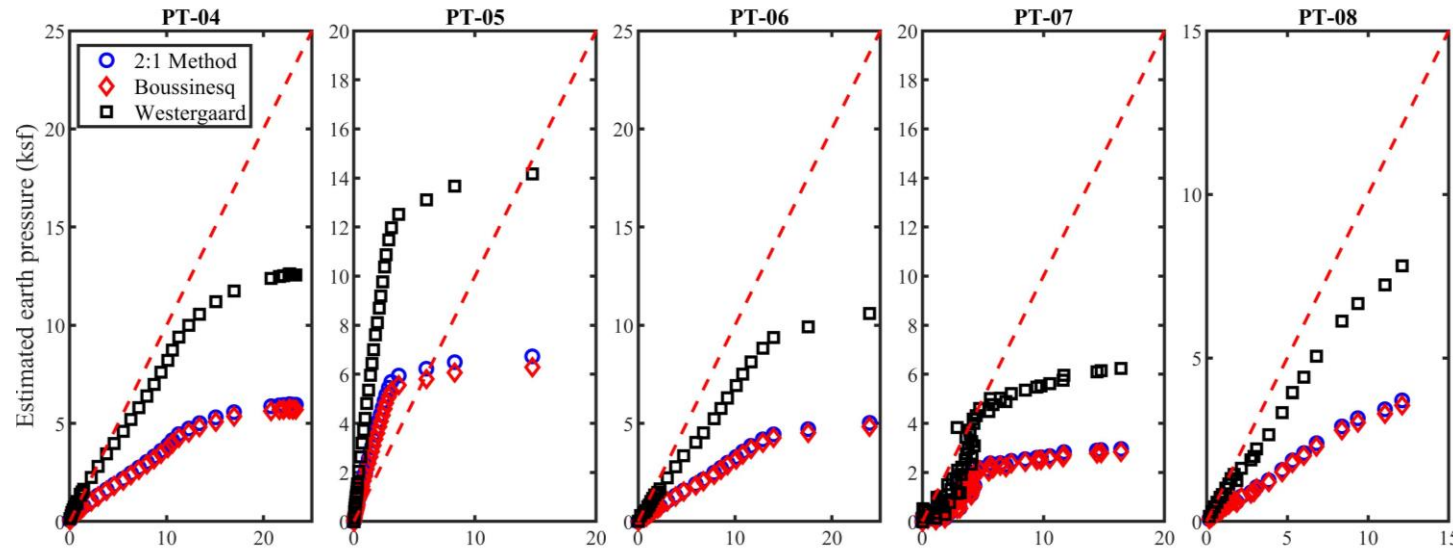
## Westergaard solution

$$\Delta\sigma_z = \frac{q}{2\pi} \left\{ \cot^{-1} \left[ \eta^2 \left( \frac{1}{m^2} + \frac{1}{n^2} \right) + \eta^4 \left( \frac{1}{m^2n^2} \right) \right]^{0.5} \right\}$$

Comparison of vertical earth pressure during loading of GRS pier up to elastic range of the stress-strain response



Comparison of vertical earth pressure during construction of GRS pier



Measured earth pressure increment (ksf)

Comparison of vertical earth pressure during loading of GRS pier

# Task 4: Comparison with design methods - reinforcement strain

## AASHTO Method

$$T_{max,i} = \sigma_H \times S_v$$

## FHWA GRS-IBS Method

$$T_{req,i} = \left( \frac{\sigma_h - \sigma_c}{0.7 \left( \frac{S_v}{6d_{max}} \right)} \right) S_v$$

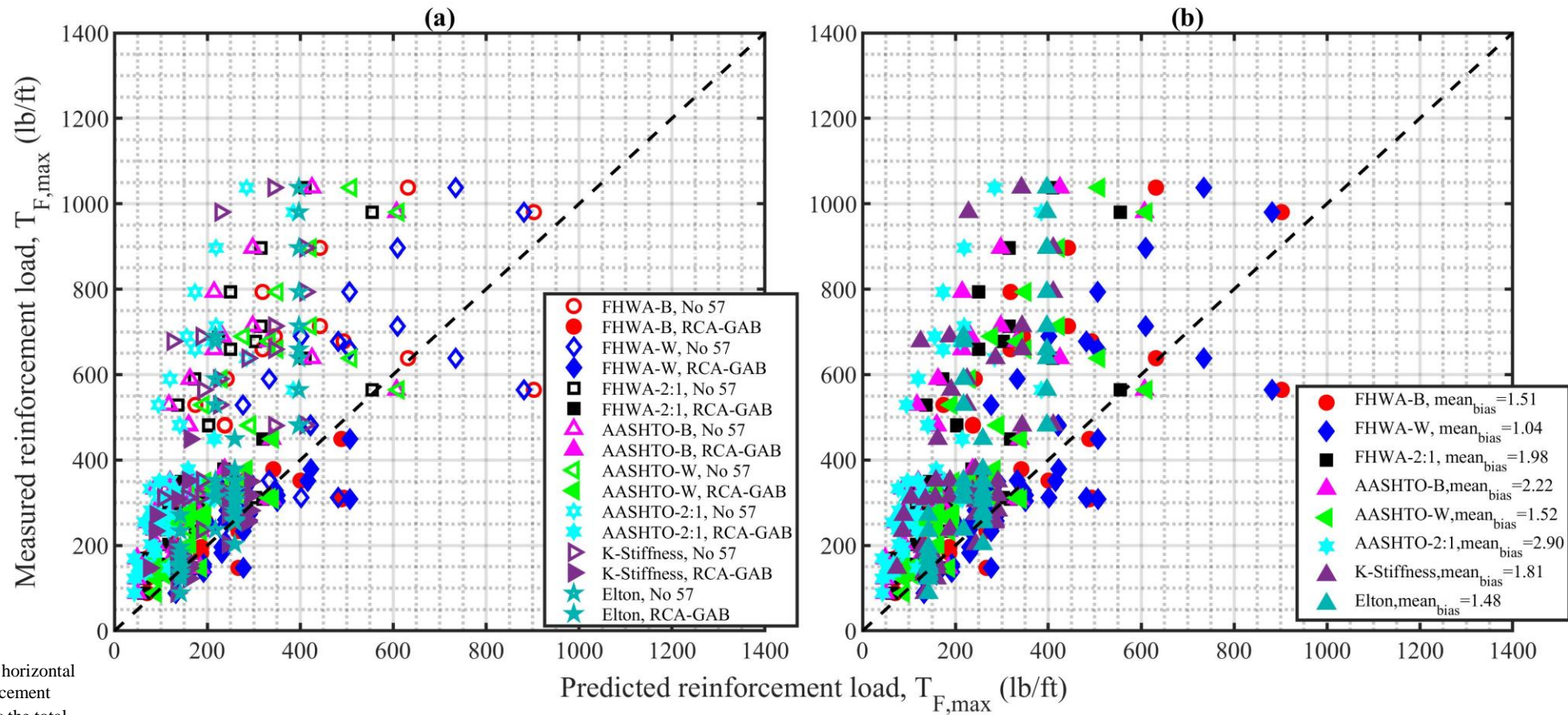
## Elton and Patawaran (2005)

$$T_{max,AU} = (\sigma_V \times K) \times S_v \times SDF$$

## K-Stiffness Method (Allen and Bathurst (2003))

$$T_{max,i} = \frac{1}{2} K \gamma (H + S) S_v^i D_{tmax} \Phi$$

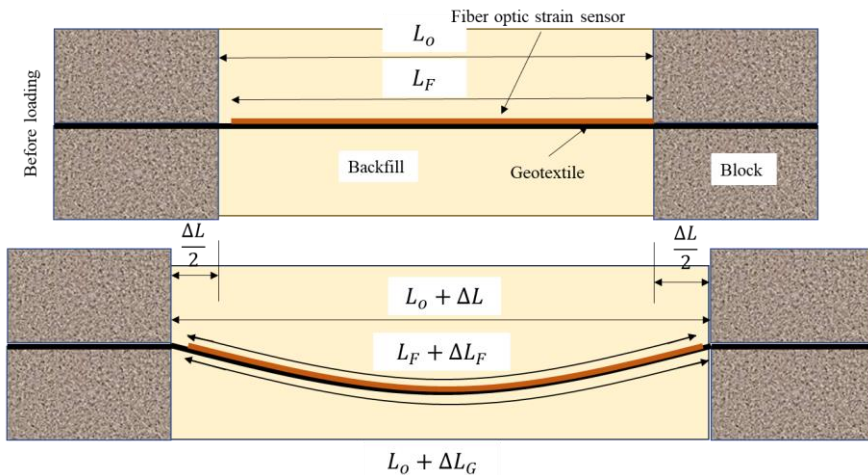
Where  $S_v$  is the vertical spacing of reinforcement,  $\sigma_h$  is the horizontal soil stress at the reinforcement,  $T_{req,i}$  is the required reinforcement strength in the direction perpendicular to the wall face,  $\sigma_h$  is the total lateral stress within the GRS composite at a given depth and location,  $\sigma_c$  is the external confining pressure,  $d_{max}$  is the maximum particle size,  $\Phi$  is the influence factor,  $D_{tmax}$  is the load distribution factor,  $S$  equivalent height of uniform surcharge pressure,  $\gamma$  is unit weight of the soil,  $H$  is height of the wall,  $K$  is lateral earth pressure coefficient, and  $SDV$  is strain distribution factor from the strain distribution curve



A plot of measured versus predicted reinforcement load. (a) Based on backfill type; (b) All combined.

( FHWA-B is from reinforcement loads based on FHWA and Boussinesq method, FHWA-W is from reinforcement loads based on FHWA and Westergaard solution, FHWA-2:1 is from reinforcement loads based on FHWA and approximate 2:1 method, AASHTO-B is from reinforcement loads based on AASHTO and Boussinesq method, AASHTO-W is from reinforcement loads based on AASHTO and Westergaard solution, and AASHTO-2:1 is from reinforcement loads based on AASHTO and approximate 2:1 method).

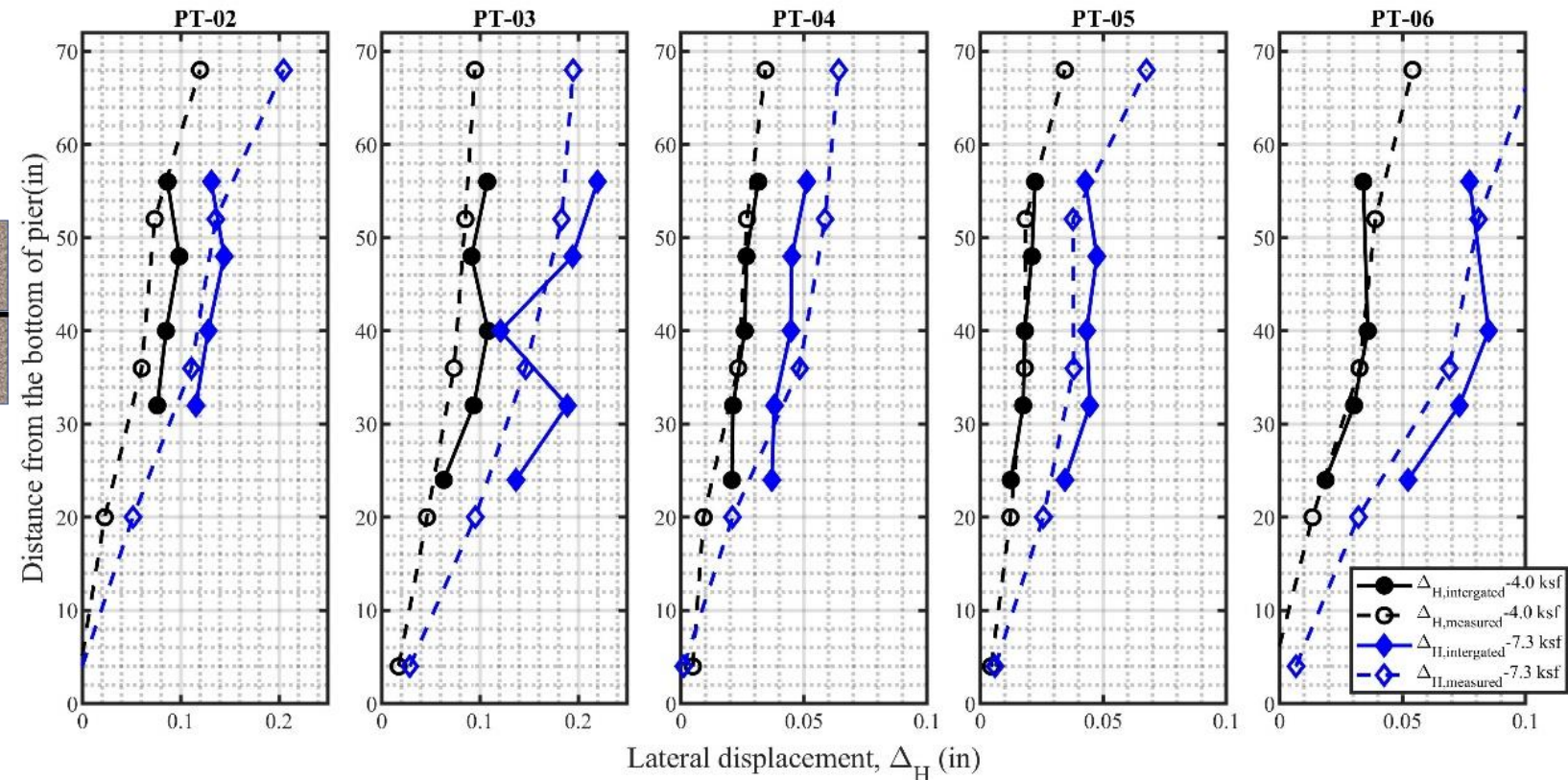
# Task 4: Comparison with design methods – measured and strain displ.



## Lateral displacement from reinforcement strain

$$\Delta H_{integrated} = \Delta L_F = \int_0^{L_F} \epsilon_r dx$$

Where  $\epsilon_r$  is the measured reinforcement strain,  $L_F$  is the total length of section that fiber optic strain sensor is being considered, and  $\Delta H_{integrated}$  is the computed lateral displacement from measured reinforcement strain.



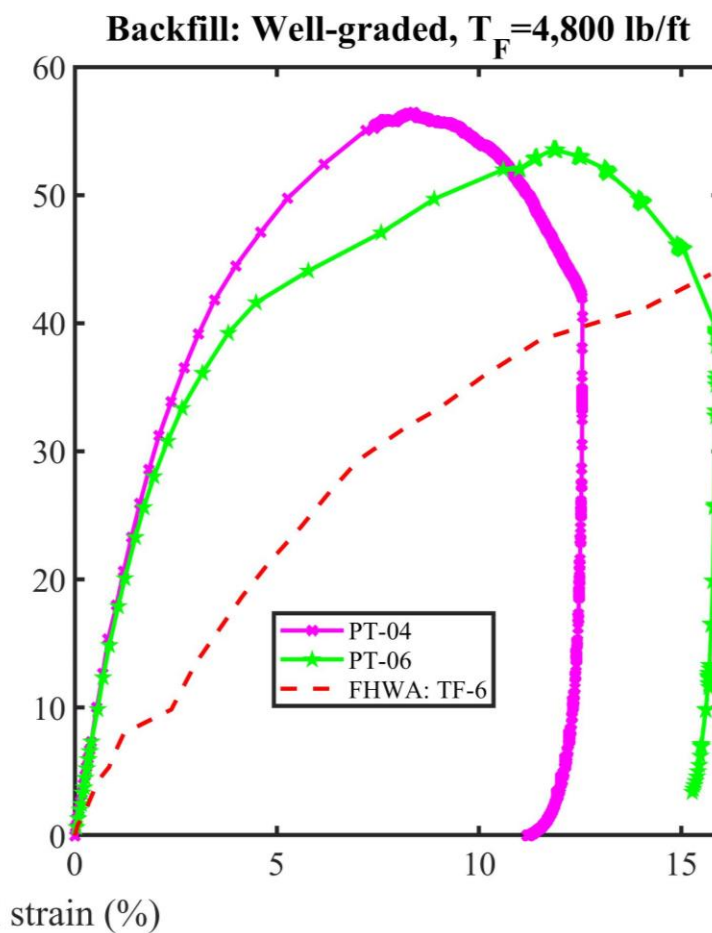
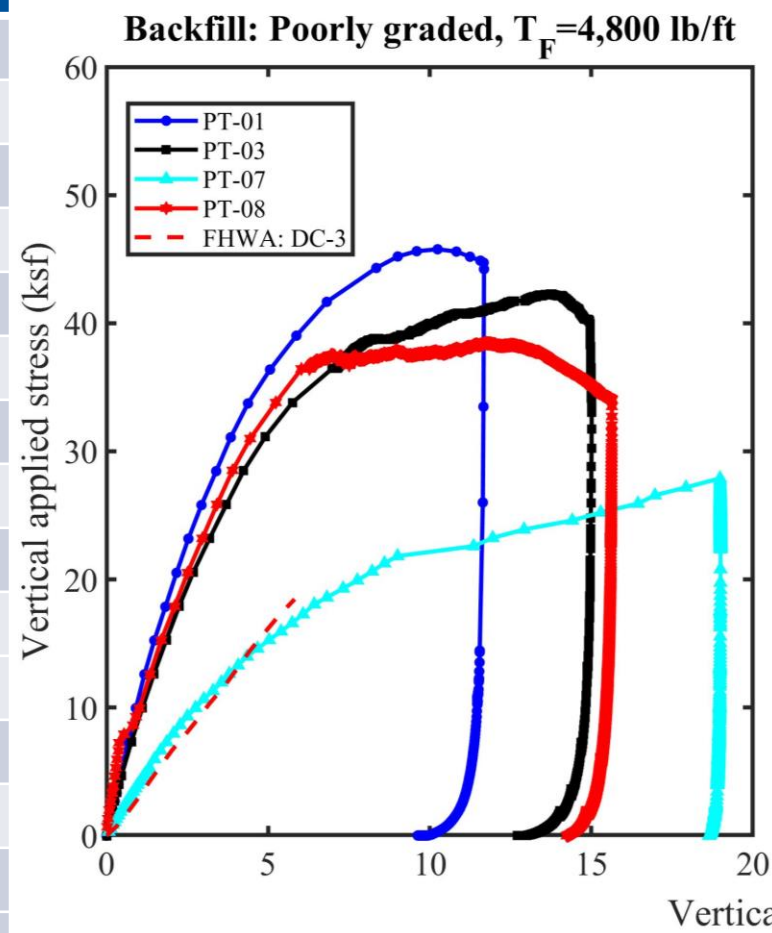
Comparison of lateral displacement estimated from the integration of reinforcement strain with measured lateral displacement at different applied vertical stresses

## Task 4: Comparison with FHWA GRS pier test data

Parameter	FDOT	FHWA ((Nicks et al, 2013))
Height (in)	72	76.25
Inside width (in)	36	39.25
$S_v$ (in)	8	8
$T_F$ (lb/ft)	4,800	4,800
Facing block type	SGR	CMU
Block size	8 x 12 x 18	7.625 x 7.625 x 15.625
Block weight (lb)	86	42
Backfill: Well graded		
Friction angle (deg)	47.3 <sup>b</sup>	54 <sup>a</sup>
Cohesion (psf)	2,148.6 <sup>b</sup>	115 <sup>a</sup>
Max dry unit weight (pcf)	115.9	148.9
Backfill: Open-graded		
Friction angle (deg)	54.4 <sup>a</sup>	52 <sup>a</sup>
Cohesion (psf)	0	0
Max dry unit weight (pcf)	96.17	108.69

<sup>a</sup> :based on 12 x12 large direct shear test

<sup>b</sup> :based on 4-inch diameter triaxial tests

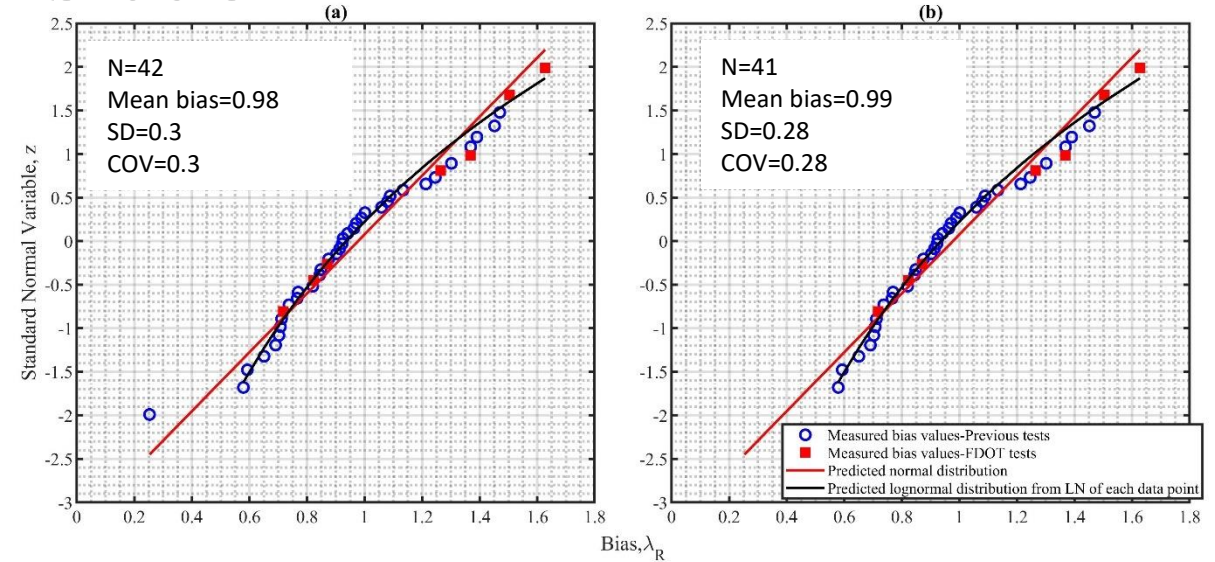


Comparison of applied vertical stress versus average vertical strain

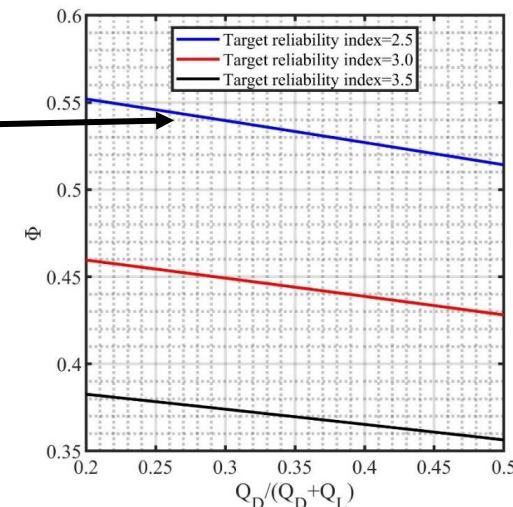
# Task 4: LRFD resistance factor calibration

- FDOT GRS-IBS design
  - Load and Resistance Factor Design (LRFD) methodology
  - Also, LRFD for all bridges that receives federal funding
- Resistance factor calibration
  - FHWA capacity equation
  - Use data from this study and from literature
  - First order second moment (FOSM) approach
- FHWA Guideline
  - FHWA guidelines use resistance factor 0.45
  - With new data from this study – resistance factor = 0.51-0.55 for target reliability of 2.5

$$\Phi = \frac{\lambda_r \left( \gamma_D \left[ \frac{Q_D}{Q_D + Q_L} \right] + \gamma_L \right)}{\left( \lambda_D \left[ \frac{Q_D}{Q_D + Q_L} \right] + \lambda_L \right) \sqrt{\frac{1 + V_R^2}{1 + V_Q^2}} e^{\left( \beta_T \sqrt{\ln[(1 + V_R^2)(1 + V_Q^2)]} \right)_i}$$

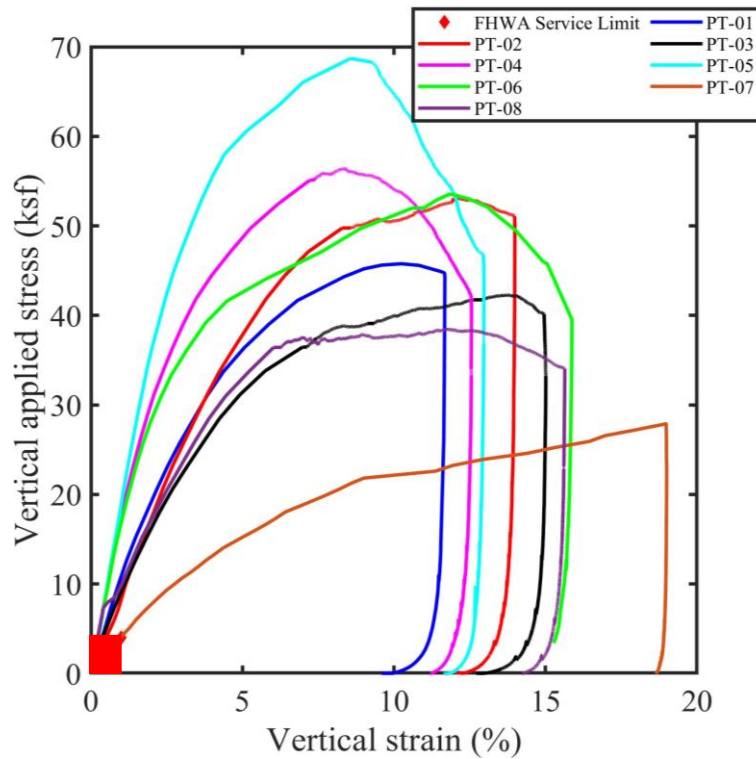


Standard normal variable as a function of bias. (a) Before removing outlier (b) After removing outlier (MP-B test from Adams et al. (2007)).

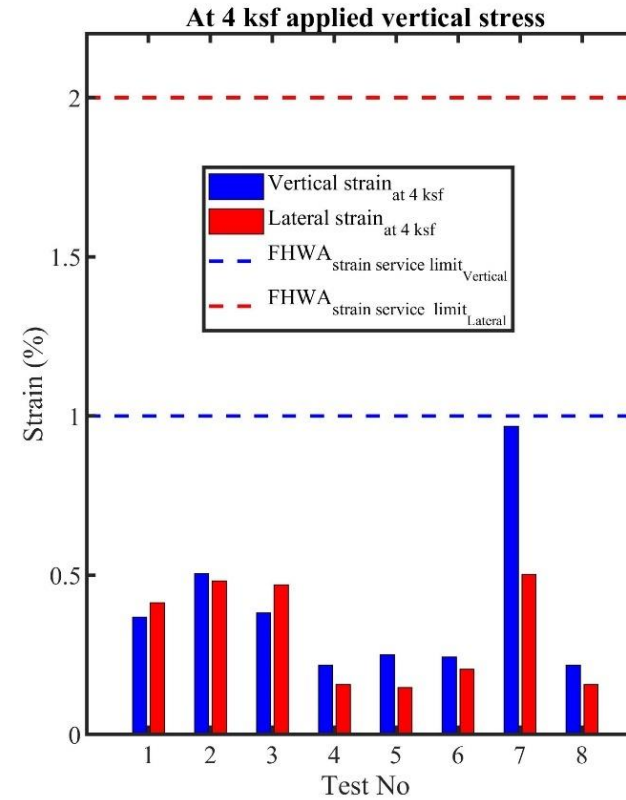


A plot of resistance factors versus dead to dead plus live load ratios for different reliability indices using all data from literature and current study

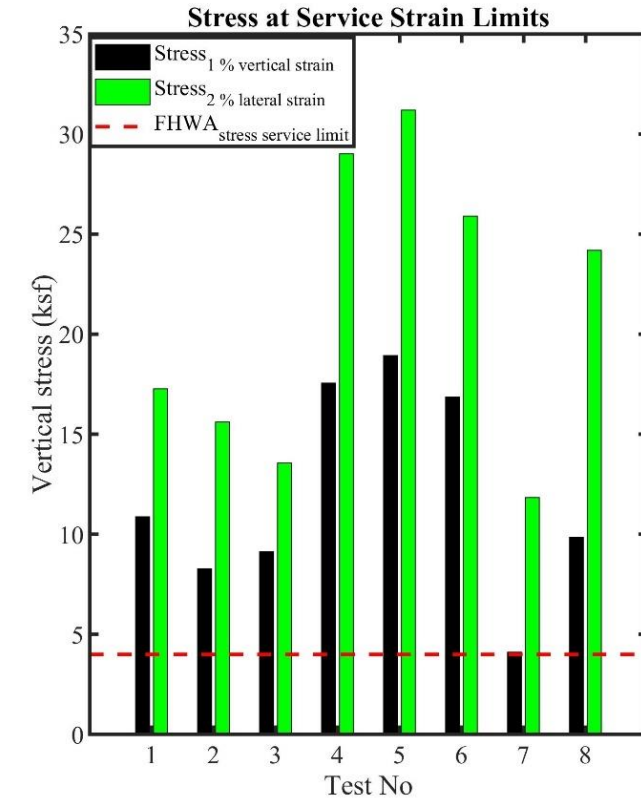
# Summary of Research Conclusions: FHWA Service Limits



Stress and vertical strain at FHWA service limits



Stress and strain at FHWA service limits



- At 1 % vertical strain
  - Applied vertical stress (4.1-19 ksf)
- At 2 % lateral strain
  - Applied vertical stress (11-32 ksf)

- GRS piers performed well at service limits

- At 4 ksf
  - Vertical strain were less than 1 %
  - Lateral strain were less than 0.51 %

## Summary of Research Conclusions

- Materials testing
  - Large triaxial tests are appropriate for testing well graded RCA-GAB backfill materials
  - Shear test strain levels should identify residual stress
  - Shear test specimen size influenced aggregate volumetric deformation and shear mobilization
- Influence of aggregate and geotextile:
  - GRS piers constructed with high strength geotextiles (HP 770(7,200 lb/ft in MD and 5,760 lb/ft in CD)) exhibited higher load capacity than those with low strength geotextiles (HP 570 and HPG 57(4,800 lb/ft in MD and CD). ).
  - GRS piers constructed with well graded RCA-GAB exhibited higher load capacity, stiffness, and less lateral displacement than those with poorly graded No 57.
  - Reinforcement tension strain distribution independent of aggregate type.
  - Less measured reinforcement tension strains in well graded RCA-GAB aggregate piers than poorly graded No 57 aggregate piers.
- Concrete fill in top three courses of facing blocks provided additional confinement increasing pier stiffness and strain performance to about twice service pressure.
- Fiber optic strain sensors capture the strain distribution in the geotextile reinforcement and survive well into elastic range of pier response.

## Summary of Research Conclusions

- The greatest strains generally developed around the center of the reinforcement layers, except in the upper layers where there was high strains near the facing blocks (highest lateral displacements before yielding).
- Integrated strain measurements can estimate lateral displacements.
- The FHWA method for lateral displacement is a good predictor for GRS piers.
- Based on the test results, the FHWA with Westergaard stress distribution method is best predictor of reinforcement tension force.
- Accurate friction angle of aggregate is most influential in the prediction of reinforcement loads.
- Resistance factor ranging from 0.51 to 0.55 for target reliability of 2.5.
- For FDOT SDG min friction angle of  $42^\circ$ , results suggest conservative estimation of GRS-IBS ultimate capacity.

## Recommendations

- Large diameter triaxial tests should be performed for aggregates to be use as compacted backfill.
- Based on the results, RCA-GAB aggregate backfill will result in good performance of GRS-IBS structures, but factors like cost, availability and ease of construction is important.
- GRS with lightweight FGA backfill performed satisfactory against the FHWA service. The results suggest additional bearing bed reinforcement, geogrid in the bearing bed, and/or cement filling of the top 3 courses of facing blocks will reduce the lateral and vertical deformations. Further tests should be conducted to explore this and the performance of a composite FGA/aggregate GRS system.
- The use of fiber optic as embedded strain sensing for long term monitoring of deformations under service conditions is promising. Fiber optic provides high resolution (10 cm) strain and temperature that is immune to electrical and chemical interference.

## Acknowledgements

- The researchers would like to thank:
  - Florida Department of Transportation (FDOT) for the financial support.
  - FDOT Marcus Structure Research Center for providing access and assistance in construction, instrumentation, and testing of the GRS piers.
  - FDOT State Material Office for their assistance in testing the materials.
  - Dr. Rawlinson at UF Structures Lab and Steven Squillicote at FAMU-FSU COE.
  - Michael Adams and Dr. Jennifer Nicks Adams at FHWA Turner-Fairbank Highway Research Center-Geotechnical Laboratory for their valuable inputs during design of the GRS piers and for conducting large direct shear tests of No 57 aggregate.



# Publications

- Axial Load Tests of Geosynthetic Reinforced Soil (GRS) Piers Constructed with Florida Limestone Aggregate and Woven Geotextile (2023): Christian Matemu<sup>1</sup>; Scott Wasman, Ph.D.<sup>2</sup>; Larry Jones<sup>3</sup>, ASCE Geo-Congress 2023, Los Angeles.
- Reinforcement Strain Measurement Using Fiber Optic Strain Sensors in Geosynthetic Reinforced Soil Piers: Christian H. Matemu<sup>1</sup>, Scott J. Wasman, Ph.D.<sup>2</sup> Eudy Steve<sup>3</sup>, Justin Robertson<sup>3</sup>, Christina Freeman<sup>3</sup>, and Larry Jones<sup>4</sup> (Drafted and Under Co-Author Review)
- Experimental Study of Geosynthetic Reinforced Soil (GRS) Piers Constructed with Florida Granular Backfill and Woven Geotextile: Christian Matemu<sup>1</sup>; Scott Wasman, Ph.D.<sup>2</sup>; Larry Jones<sup>3</sup> (Drafted and Under Co-Author Review)
- Influence of backfill properties on the performance of Geosynthetic Reinforced Soil (GRS) Piers : Christian Matemu<sup>1</sup>; Scott Wasman<sup>2</sup> (Under preparation)
- Numerical Modeling of GRS piers under different facing conditions: Christian Matemu<sup>1</sup>; Scott Wasman<sup>2</sup> (Under preparation)
- Performance of Lightweight Aggregate Backfilled Geosynthetic Reinforced Soil (GRS) Piers Under Axial Load: Christian H. Matemu, Ph.D.<sup>1</sup>, Joshua Vincent<sup>2</sup>, Scott Wasman, Ph.D.<sup>3</sup> and Larry Jones<sup>4</sup>, ASCE Geo-Congress 2025, Louisville.
- Axial Load Tests of Geosynthetic Reinforced Soil Piers Constructed with Florida Limestone and Recycled Concrete Aggregates: Scott Wasman, Christian Matemu, Larry Jones, Transportation Research Board Conference 2023, Standing Committee on Transportation Earthworks (AKG50), Washington, D.C.

### Axial Load Tests of Geosynthetic Reinforced Soil (GRS) Piers Constructed with Florida Limestone Aggregate and Woven Geotextile

Christian H. Matemu<sup>1</sup>, Scott J. Wasman, Ph.D.<sup>2</sup>, and Larry Jones<sup>3</sup>

<sup>1</sup>Dept. of Civil and Coastal Engineering, Univ. of Florida, Gainesville, FL.

<sup>2</sup>Dept. of Civil and Environmental Engineering, FAMU-FSU College of Engineering, Florida State Univ., Tallahassee, FL. Email: swasman@eng.famu.fsu.edu

<sup>3</sup>Florida Dept. of Transportation, Tallahassee, FL. Email: Larry.Jones@dot.state.fl.us

#### ABSTRACT

Full-scale tests on instrumented geosynthetic reinforced soil (GRS) piers were performed to investigate geosynthetic stiffness and strength influence on axial load-deformation performance. Each pier was constructed with poorly graded Florida limestone aggregate, segmental facing blocks, and basal woven polypropylene geotextile. The vertical displacement of the top of the pier, the deflected shape, and tensile strains in the reinforcement were monitored during the test. Results indicate the position of maximum lateral displacement shifts from the top to two-thirds of the wall height as the load increases. Measured reinforcement strains are greatest in the middle layers of the pier. At the upper layers, the reinforcement strains are greater close to the edge of the blocks, while at the middle layers they are greater at the center of the geotextile. Stress-strain curves developed from the measurements show ultimate bearing capacities are 17%–36% greater than the predictions using the FHWA recommended equation.

### Experimental Study of Geosynthetic Reinforced Soil (GRS) Piers Constructed with Florida Aggregate Backfill and Woven Geotextile

Christian H. Matemu<sup>1</sup>, Scott J. Wasman, Ph.D.<sup>2</sup> and Larry Jones<sup>3</sup>

<sup>1</sup>Department of Civil and Coastal Engineering, University of Florida, P.O. Box 98765, Gainesville, FL 32611-1111; E-mail: christian.matemu@ufl.edu

<sup>2</sup>Department of Civil and Environmental Engineering, FAMU-FSU College of Engineering, Florida State University, P.O. Box 3062870, Tallahassee, FL 32310. E-mail: swasman@eng.famu.fsu.edu

<sup>3</sup>Florida Department of Transportation, 605 Suwannee St., Tallahassee, FL 32399; E-mail: Larry.Jones@dot.state.fl.us

#### ABSTRACT

This paper presents the results of an experimental study that involved six full-scale tests of Geosynthetic Reinforced Soil (GRS) piers. The study aimed to investigate influence of open graded and well graded aggregate backfill reinforced with different gradations on the load bearing and deformation behavior of GRS structures. The study found that backfill with higher strength geotextile and backfill have greater loading capacity and compared to those with lower strength materials. The maximum lateral displacement reinforcement strain were observed in the top one-third and upper half of the wall respectively. Additionally, the highest strain values were found closer to the connection of the upper layers, while they were located near the middle for the lower layers. The Highway Administration (FHWA) ultimate capacity equation was found to underestimate bearing capacity, suggesting the bearing bed reinforcement and the type of face are measurable contributors to design capacity and a need for further investigation. Also the assumption of zero volume change was found to hold only below the FHWA test bearing pressure of 191.5 kPa.

### Performance of Lightweight Aggregate Backfilled Geosynthetic Reinforced Soil (GRS) Piers Under Axial Load

Scott Wasman, Ph.D.<sup>1</sup>, Joshua Vincent<sup>2</sup>, Christian H. Matemu<sup>3</sup>

<sup>1</sup>Department of Civil and Environmental Engineering, FAMU-FSU College of Engineering, Florida State University, P.O. Box 3062870, Tallahassee, FL 32310; Corresponding author e-mail: swasman@eng.famu.fsu.edu

<sup>2</sup>Department of Civil and Environmental Engineering, FAMU-FSU College of Engineering, Florida State University, P.O. Box 3062870, Tallahassee, FL 32310; E-mail: jvc21@fsu.edu

<sup>3</sup>Department of Civil and Coastal Engineering, University of Florida, P.O. Box 98765, Gainesville, FL 32611-1111; E-mail: christian.matemu@ufl.edu

#### ABSTRACT

Full-scale tests on instrumented geosynthetic reinforced soil (GRS) piers were performed to investigate the bearing and deformation performance of backfill composed of lightweight aggregate and composite 40/60 proportion lightweight aggregate and poorly graded aggregate, respectively. Each pier was constructed with a height to width ratio of 2 and confined with concrete masonry unit blocks. The reinforcement was a woven polypropylene geotextile with 4,800 lbf tensile strength in the machine and cross-machine directions. The applied load, vertical displacement of a footing atop the pier, and the deflected shape of each pier was monitored during the tests. Results indicate the capacity and deformations of the lightweight aggregate backfilled pier to meet recommended service limits. Furthermore, the composite backfill of lightweight aggregate and poorly graded aggregate increase the capacity and stiffness response of the pier, but it limited based on the lightweight fracturing and crushing under higher stresses, conditions the position of maximum lateral displacements shifts from the top to two-thirds of the wall height as the load increases.

### Reinforcement Strain Measurement Using Fiber Optic Strain Sensors in Geosynthetic Reinforced Soil Piers

Christian H. Matemu<sup>1</sup>, Scott J. Wasman, Ph.D.<sup>2</sup>, Stephen Eudy<sup>3</sup>, Justin Robertson<sup>3</sup>, Christina Freeman<sup>3</sup>, and Larry Jones<sup>4</sup>

<sup>1</sup>Department of Civil and Coastal Engineering, University of Florida, P.O. Box 98765, Gainesville, FL 32611

<sup>2</sup>Department of Civil and Environmental Engineering, FAMU-FSU College of Engineering, Florida State University, P.O. Box 3062870, Tallahassee, FL 32310

<sup>3</sup>Florida Department of Transportation, FDOT M.H. Anderson Structures Research Center, 2007 E. Paul Dirac Dr., Tallahassee, FL, 32310

<sup>4</sup>Florida Department of Transportation, 605 Suwannee St., Tallahassee, FL 32399

#### ABSTRACT

Development of tensile strains in the geosynthetics of reinforced soil systems is important for the internal stability and the reliable performance of the load carrying composite system. In studies of full-scale reinforced soil systems, measurements of tensile strain are usually made with strain gauges that are bonded to the reinforcement. To obtain a strain distribution, multiple gauges are necessary, and with these are the multiple wires for each gauge. This makes the measurement setup tedious and can introduce interference with the reinforcement mechanism provided by the geosynthetic. To overcome this, this paper introduces a new approach that utilizes fiber optic strain sensors for measuring reinforcement strain in geosynthetic reinforced soil systems. The use of fiber optic strain sensors offers several advantages such as high accuracy, immunity to electromagnetic interference, simplicity in installation, and the ability to assure multiple points simultaneously. The procedures for installing and calibrating the fiber optic strain sensors are presented, and the results from the strain measurements are compared to those from strain gauges. Measured tensile forces are compared to design methods, applied AASHTO, FHWA, for GRS-BIS, K-Stiffness, and Elbow and Patrawara's methods, results suggest the use of fiber optic strain sensors is effective in measuring the reinforcement strain in reinforced soil mass.

### Influence of Backfill Strength Properties on Performance of Geosynthetic Reinforced Soil Piers

Christian H. Matemu<sup>1</sup>, Scott J. Wasman, Ph.D.<sup>2</sup>, David Horhota, Ph.D.<sup>3</sup>, Christina Freeman<sup>4</sup>, and Larry Jones<sup>5</sup>

<sup>1</sup>Department of Civil and Coastal Engineering, University of Florida, P.O. Box 98765, Gainesville, FL 32611-1111; E-mail: christian.matemu@ufl.edu

<sup>2</sup>Department of Civil and Environmental Engineering, FAMU-FSU College of Engineering, Florida State University, P.O. Box 3062870, Tallahassee, FL 32310; E-mail: swasman@eng.famu.fsu.edu

<sup>3</sup>Florida Department of Transportation, State Materials Office, 5007 NE 39th Ave, Gainesville, FL 32609; E-mail: david.horhota@dot.state.fl.us

<sup>4</sup>Florida Department of Transportation, FDOT M.H. Anderson Structures Research Center, 2007 E. Paul Dirac Dr., Tallahassee, FL, 32310

<sup>5</sup>Florida Department of Transportation, 605 Suwannee St., Tallahassee, FL 32399; E-mail: Larry.Jones@dot.state.fl.us

#### ABSTRACT

This paper presents an experimental study aimed at assessing the strength characteristics of Florida aggregates backfill and the performance of five geosynthetic reinforced soil (GRS) piers constructed using various backfill and reinforcement materials, as well as different pier configurations. Three types of aggregates were used as structural backfill, while two types of woven polypropylene geotextiles were used for reinforcement. Segmental retaining blocks were used for constructing facing walls. Two pier configurations were considered, with and without concrete fill at the top course. The study revealed that graded aggregate base-recycled aggregate (RCA-GAB) exhibited higher friction and dilation angles compared to No 57 limestone during triaxial testing. Additionally, the scalping of larger materials had a lesser

### Performance of Lightweight Aggregate Backfilled Geosynthetic Reinforced Soil (GRS) Piers Under Axial Load

Christian H. Matemu, Ph.D.<sup>1</sup>, Joshua Vincent<sup>2</sup>, Scott Wasman, Ph.D.<sup>3</sup> and Larry Jones<sup>4</sup>

<sup>1</sup>Department of Civil and Coastal Engineering, University of Florida, P.O. Box 98765, Gainesville, FL 32611-1111; E-mail: christian.matemu@ufl.edu

<sup>2</sup>Department of Civil and Environmental Engineering, FAMU-FSU College of Engineering, Florida State University, P.O. Box 3062870, Tallahassee, FL 32310; E-mail: jvc21@fsu.edu

<sup>3</sup>Department of Civil and Environmental Engineering, FAMU-FSU College of Engineering, Florida State University, P.O. Box 3062870, Tallahassee, FL 32310; E-mail: swasman@eng.famu.fsu.edu

<sup>4</sup>Florida Department of Transportation, 605 Suwannee St., Tallahassee, FL 32399; E-mail: Larry.Jones@dot.state.fl.us

#### ABSTRACT

Full-scale tests on instrumented geosynthetic reinforced soil (GRS) piers were performed to investigate the bearing and deformation performance of lightweight aggregate and a poorly graded No. 57 stone backfill. Each pier was constructed with a height to width ratio of 2 and confined with segmental retaining blocks. The reinforcement was a woven polypropylene geotextile with 105 kN/m and 84 kN/m tensile strengths in the machine direction (MD) and cross-machine direction (CD), respectively, and vertically spaced 0.2 meters. The applied load, vertical displacement of a footing at the top of the pier, and the deflected shape of each pier were monitored during the tests. Results indicate the capacity and deformations of the lightweight aggregate backfilled pier to meet recommended service limits and to be about 40% of the load carried by the No. 57 stone pier at 1% vertical strain. Yielding of the lightweight aggregate pier is around 2% axial strain followed by aggregate crushing within the top third of the pier and a bearing capacity of about two-thirds of the No. 57 stone pier.

## References

- Adams, M., Nicks, J. (2018). Design and Construction Guidelines for Geosynthetic Reinforced Soil Abutments and Integrated Bridge Systems, Report No. FHWA-HRT-17-080. Federal Highway Administration, Washington, DC.
- Adams, M.T., Nicks, J.E., Stabile, T., Wu, J.T.H., Schlatter, W., and Hartmann, J. (2012). Geosynthetic Reinforced Soil Integrated Bridge System Interim Implementation Guide, Report No. FHWA-HRT-11-026, Federal Highway Administration, Washington, DC.
- Allen, T. M., & Bathurst, R. J. (2003). Prediction of reinforcement loads in reinforced soil walls (No. Final Research Report,). Washington State Transportation Center (TRAC).
- Daniyarov, A., Zelenko, B., Derian, A., 2017. Deployment of the Geosynthetic Reinforced Soil Integrated Bridge System from 2011 to 2017, Report No. FHWA-HIF-17-043. Federal Highway Administration, Washington, DC.
- Das, B.M., 2019. Advanced soil mechanics. CRC press.
- Doger, R., 2020. Influence of Facing on the Construction and Structural Performance of GRS Bridge Abutments. The University of Oklahoma.
- Elton, D. J., & Patawaran, M. A. B. (2005). Mechanically stabilized earth (MSE) reinforcement tensile strength from tests of geotextile reinforced soil. Alabama Highway Research Center, Auburn University.
- FDOT, 2020. Standard specifications for road and bridge construction. Florida DOT Tallahassee, FL.
- FDOT. (2021). Structures Manual: Volume 1 – Structures Design Guidelines.
- Lwamoto, M.K., 2014. Observations from load tests on geosynthetic reinforced soil. University of Hawaii at Manoa.
- Matemu, C. H., Wasman, S. J., & Jones, L. Axial Load Tests of Geosynthetic Reinforced Soil (GRS) Piers Constructed with Florida Limestone Aggregate and Woven Geotextile. In Geo-Congress 2023 (pp. 369-378).
- Nicks, J.E., Adams, M., Ooi, P., Stabile, T., 2013. Geosynthetic reinforced soil performance testing—Axial load deformation relationships, Report No. FHWA-HRT-13-066. Federal Highway Administration- Research, Development and Technology, McLean, VA.
- Wu, J. T. H. (2019). Characteristics of geosynthetic reinforced soil (GRS) walls: an overview of field-scale experiments and analytical studies. Transportation Infrastruct. Geotechnol. 6 (2), 138–163 (2019).

Thank You!